

Characterization of ScAP-23, a new cell line from murine subcutaneous adipose tissue, identifies genes for the molecular definition of preadipocytes

Ji Young Kim, Yu Wu and Cynthia M. Smas

Physiol. Genomics 31:328-342, 2007. First published 3 July 2007;
doi:10.1152/physiolgenomics.00206.2006

You might find this additional info useful...

Supplemental material for this article can be found at:

<http://physiolgenomics.physiology.org/content/suppl/2007/08/15/00206.2006.DC1.html>

This article cites 126 articles, 67 of which can be accessed free at:

<http://physiolgenomics.physiology.org/content/31/2/328.full.html#ref-list-1>

This article has been cited by 1 other HighWire hosted articles

Adipose triglyceride lipase and the lipolytic catabolism of cellular fat stores

Rudolf Zechner, Petra C. Kienesberger, Guenter Haemmerle, Robert Zimmermann and Achim Lass

J. Lipid Res., January , 2009; 50 (1): 3-21.

[\[Abstract\]](#) [\[Full Text\]](#) [\[PDF\]](#)

Updated information and services including high resolution figures, can be found at:

<http://physiolgenomics.physiology.org/content/31/2/328.full.html>

Additional material and information about *Physiological Genomics* can be found at:

<http://www.the-aps.org/publications/pg>

This information is current as of October 21, 2011.

Characterization of ScAP-23, a new cell line from murine subcutaneous adipose tissue, identifies genes for the molecular definition of preadipocytes

Ji Young Kim, Yu Wu, and Cynthia M. Smas

Department of Biochemistry and Cancer Biology, University of Toledo Health Science Campus, Toledo, Ohio

Submitted 19 September 2006; accepted in final form 26 June 2007

Kim JY, Wu Y, Smas CM. Characterization of ScAP-23, a new cell line from murine subcutaneous adipose tissue, identifies genes for the molecular definition of preadipocytes. *Physiol Genomics* 31: 328–342, 2007. First published July 3, 2007; doi:10.1152/physiolgenomics.00206.2006.—The 3T3-L1 model of in vitro adipogenesis has provided key insights into the molecular nature of this process. However, given that 3T3-L1 are of an embryonic origin, it is not clear to what extent they represent adipogenesis as it occurs in white adipose tissue (WAT). With the goal of better defining preadipocytes and adipogenesis in WAT, we have generated a new cell culture model from adipocyte precursors present in C57BL/6 mouse subcutaneous WAT. ScAP-23 preadipocytes show fibroblastic morphology, and on treatment with dexamethasone, 3-methylisobutylxanthine, insulin, and indomethacin, convert to nearly 100% adipocyte morphology. ScAP-23 adipocytes contain abundant lipid droplets and express transcripts for PPAR γ , C/EBP family, and SREBP-1c transcription factors, SCD1, aFABP, ATGL, GLUT4, FAS, LDL, and GPDH, and are insulin responsive. Differential screening of 1,176 genes using nylon DNA arrays identified 10 transcripts enriched in ScAP-23 adipocytes vs. preadipocytes and 26 transcripts enriched in ScAP-23 preadipocytes vs. adipocytes. Semi-quantitative or real-time PCR analyses identified a common cohort of 14 transcripts markedly downregulated in both ScAP-23 and 3T3-L1 adipogenesis. These included catenin- β 1, chemokine ligand-2, serine or cysteine peptidase inhibitor f1, aurora kinase B, thrombospondin2, and solute carrier-7a5. Five of these transcripts (Ccl2, Serpinf1, Aurkb, Thbs2, and Slc7a5) demonstrated at least a twofold increase in WAT from obese (*ob/ob*) mice compared with that of wild-type mice. This suggests that comparative gene expression studies of ScAP-23 and 3T3-L1 adipogenesis may be particularly fruitful in identifying preadipocyte-expressed genes that play a role in adipose tissue physiology and/or pathophysiology.

differentiation; adipogenesis; immortalization; subcutaneous adipocyte precursor

THE PRIMARY ROLE OF white adipose tissue (WAT) is the storage of excess energy in adipocytes and mobilization of these reserves to meet the energy demands of the organism. Adipocytes also synthesize and secrete a number of soluble factors including leptin, resistin, and TNF α (10, 21, 39, 40, 58, 118). Excess expansion of adipose tissue mass underlies obesity and is a major health concern in modern society. Comorbidities of obesity include type 2 diabetes, hypertension, and some types of cancer (1, 12, 117). Studies on the molecular aspects of adipocyte differentiation and the examination of the function of various adipocyte-expressed gene products have yielded many advances in the last several decades (40, 46, 67, 72, 81). These have led to a marked enhancement of our understanding of the

cellular and molecular basis of adipose tissue growth in physiological and pathological conditions and have provided insights into therapeutic strategies for the treatment and prevention of obesity (13, 63). Increases in WAT mass can occur via an increase in adipocyte size and/or increase in adipocyte cell number (39, 40). Adipogenesis, defined as the differentiation of preadipocyte to mature adipocyte, is ongoing throughout the lifespan and is accompanied by dramatic increases in genes that encode molecules central to adipogenesis including those critical in lipogenesis, lipolysis, lipid transport, and hormone signaling (40).

Adipose tissue precursors that can give rise to mature adipocytes in vivo remain ill defined. As such, the 3T3-L1 preadipocyte cell line (38) has served as an extensively utilized cell culture model. Studies with these cells have been key to dissecting signals controlling adipogenesis, for example the central role of the peroxisome proliferator-activated receptor- γ (PPAR γ) and C/EBP transcription factors (67, 109, 112), as well as for the functional characterization of many adipocyte-expressed genes (40, 72). However, while 3T3-L1 cells appear to recapitulate many key aspects of adipogenesis, the advent of microarray technology has allowed for a more refined molecular assessment of the relative similarities and distinctions between in vitro adipogenesis exemplified by 3T3-L1 cells vs. adipogenesis as it may occur in vivo (94). Moreover, the embryonic source of Swiss 3T3 cells, from which the 3T3-L1 cell line was generated (38), corresponds to a time in murine development at which WAT has not yet appeared (3). As such, the lineage relationship of 3T3-L1 cells to preadipocytes present in adult WAT is at present undetermined. Studies on in vivo adipogenesis have identified genes enriched in the stromal-vascular fraction of adipose tissue, compared with the adipocyte fraction (34, 94, 106). Given, however, the heterogeneous cell types present in the nonadipocyte fraction of adipose tissue, cells of the stromal-vascular population are unlikely to precisely reflect preadipocyte gene expression and/or phenotype. In addition, it has been reported that a multitude of gene expression changes occur as a result of standard procedures used in fractionation of adipose tissue into adipocyte and stromal-vascular cell fractions (85). Thus the need to develop and utilize additional models for in vitro adipogenesis studies to complement studies in 3T3-L1 cells is increasingly evident; several of these alternate models have already proven useful in the study of adipogenesis and adipocyte gene expression (28, 49, 51, 56, 77, 110, 119). Overall, the ability to use new and/or multiple adipogenesis models should greatly facilitate a further refinement of the definition of that cohort of genes that most centrally define the preadipocyte and adipocyte phenotype. Furthermore, uncovering the distinct characteristics of individual adipogenesis models may provide unique insights into the nature of adipogenesis in, for example,

Article published online before print. See web site for date of publication (<http://physiolgenomics.physiology.org>).

Address for reprint requests and other correspondence: C. M. Smas, Dept. of Biochemistry and Cancer Biology, Univ. of Toledo Health Science Campus, Toledo, OH 43614 (e-mail: cynthia.smas@utoledo.edu).

normal vs. disease states, bone marrow vs. adipose tissue, and visceral vs. subcutaneous adipose tissue; studies that illuminate the latter process have recently been reported (34, 106).

In this study, we have developed and characterized a new, permanent preadipocyte cell line from mouse subcutaneous WAT that we designate subcutaneous adipocyte precursor, cell line-23 (ScAP-23). We have used this novel in vitro adipogenesis model to identify new differentiation-dependent genes whose expression is upregulated or abolished in adipogenesis. We believe that ScAP-23 cells will serve as a valuable new tool for the study of adipogenesis in general, and that these cells may be particularly suited for studies of the characteristics of preadipocytes and adipocytes from subcutaneous WAT.

MATERIALS AND METHODS

Fractionation of adipose tissue and establishment of the ScAP-23 preadipocyte cell line. Subcutaneous adipose tissue was removed from 3-wk-old male C57BL/6 mice, rinsed three times in sterile Hanks' balanced salt solution (HBSS), and minced with scissors. Tissue was transferred to a 50-ml sterile tube with 15 ml of HBSS containing 0.1 mg/ml type II collagenase (Sigma-Aldrich, St. Louis, MO). After digestion for 40 min at 37°C with constant agitation, material was filtered through a 250 μ m-pore size nylon mesh (Sefar America, Depew, NY), and filtrate was centrifuged at 2,000 rpm for 5 min. The floating adipocyte fraction was removed, and the pellet of preadipocyte-containing stromal-vascular cells was resuspended in DMEM containing 10% FCS and plated. This cellular fractionation protocol for adipose tissue had been validated in our hands by assessment for marker transcripts for the stromal-vascular fraction and adipocyte fraction. We also failed to detect by Northern blot transcript expression for the macrophage marker *emr1* and for the endothelial marker von Willebrand factor in these cell populations, indicating a low contribution of these cell types to our stromal-vascular fraction preparations (data not shown). For immortalization of subcutaneous stromal-vascular cells, the pBabe-puro-hTERT retroviral expression construct (kindly provided by Dr. R. Weinberg, Massachusetts Institute of Technology, Cambridge, MA) was transfected into Phoenix 293T retroviral packaging cells using the CaPO₄ coprecipitation method. After 48 h, supernatant containing retroviral particles was collected and passed through a 45- μ m filter. Stromal-vascular cells from subcutaneous adipose tissue were infected with viral supernatant in the presence of 4 μ g/ml polybrene (Sigma-Aldrich) for 6 h. Medium was changed 48 h postinfection, and cells were treated with 1 μ g/ml puromycin (Sigma-Aldrich) for 5 days to select drug-resistant cells. Cultures were expanded in DMEM containing 10% FCS and observed for spontaneous adipogenic conversion. Individual clonal lines derived thereof were tested for adipogenic conversion by treatment with various combinations of adipogenic inducing agents.

Cell culture and differentiation treatments. ScAP-23 cells were maintained in DMEM supplemented with 10% calf serum, 1% penicillin-streptomycin, and 1% glutamine and passaged before reaching confluence. Unless otherwise noted, for differentiation of ScAP-23 cells, cells were treated at confluence with DMEM supplemented with 10% FCS in the presence of the adipogenic inducers, 0.5 mM methylisobutylxanthine (MIX), 1 μ M dexamethasone, 17 nM insulin, and 0.2 mM indomethacin, for 72 h. Adipogenic agents were then removed, and cultures continued in DMEM containing 10% FCS and 17 nM insulin. At 5 days postinduction of differentiation, adipocyte conversion had occurred in nearly all cells, as judged by lipid accumulation. Earlier-stage cells (approximately up to 100 doublings) and later-stage cells (~140 doublings) readily differentiated based on morphology and on the expression of several adipocyte marker transcripts. 3T3-L1 cells (American Type Culture Collection, Manassas, VA) were propagated in DMEM supplemented with 10% calf serum. For differentiation, 3T3-L1 cells were treated at 2 days

postconfluence with DMEM supplemented with 10% FCS in the presence of the adipogenic inducers, 0.5 mM MIX and 1 μ M dexamethasone, for 48 h. Adipogenic agents were then removed, and growth of cultures continued in DMEM containing 10% FCS. At 5 days postinduction of differentiation, adipocyte conversion had occurred in nearly all cells. For assessment of multilineage differentiation of ScAP-23, we employed previously published protocols for neurogenesis (70, 86), myogenesis (124, 126), and osteogenesis (70, 86).

For Oil Red O staining, cells were rinsed twice with PBS and fixed in 10% formaldehyde in PBS for 1 h. An Oil Red O stock solution of 0.5% in isopropyl alcohol was diluted with water at a 3:2 ratio and filtered through a 0.45- μ m filter. Fixed cells were stained for 1 h at room temperature. Cells were rinsed three times with distilled water, and images were documented with an Olympus IX70 inverted microscope and a digital camera. To quantify intracellular lipid content, Oil Red O stain was extracted with isopropanol, and absorbance was measured at 510 nm and values corrected against cell number. For assessment of cell growth kinetics, ScAP-23 cells and 3T3-L1 cells were plated in six-well plates at 5×10^4 cells/well. At 24, 48, 72, 96, and 120 h following plating, cells were trypsinized and counted using a cell counting chamber. These studies were conducted three independent times; within each study, time points were assessed in triplicate.

Northern blot and DNA filter array hybridizations. RNA was isolated using an SV total RNA isolation kit (Promega, Madison, WI) for ScAP-23 cells or Trizol reagent (Invitrogen, Carlsbad, CA) for other cells and tissues, according to the manufacturer's instructions. For studies of gene expression in murine WAT, 8-wk-old C57BL/6 or *ob/ob* male mice were utilized. All animal treatments were conducted with the approval of the University of Toledo Health Science Campus Institutional Animal Care and Use Committee. Northern blot analyses were conducted a minimum of two times. For this, 5 μ g of RNA were fractionated in 1% agarose-formaldehyde gels in MOPS buffer and transferred to Hybond-N membrane (GE Healthcare, Piscataway, NJ). Blots were hybridized in ExpressHyb solution (BD Biosciences Clontech, Palo Alto, CA) with ³²P-labeled random-primed DNA probes. After a washing, membranes were exposed at -80°C to Kodak Biomax film with a Kodak Biomax intensifying screen. For quantitation of gene expression depicted in Northern blots, samples were also subject to analysis by real-time PCR. Northern blot data presented as contiguous lanes and shown as an inclusive panel arose from a single original image of a Northern blot gel and autoradiogram. However, as noted in the respective figure legend, in some instances data lanes were removed or rearranged for clarity or economy of presentation.

For DNA filter array analysis, Atlas 1.2 mouse II nylon membranes (BD Biosciences Clontech) containing 1,176 genes were hybridized with reverse-transcribed ³²P-labeled cDNA probes from ScAP-23 preadipocytes, ScAP-23 adipocytes, 3T3-L1 preadipocytes, and 3T3-L1 adipocytes. Hybridization was performed exactly per manufacturer's instructions, and membranes were exposed at -80°C to Kodak Biomax film with a Kodak Biomax intensifying screen. Following visual assessment to identify candidate genes that were either up- or downregulated in ScAP-23 adipogenesis, all candidate gene expression results reported in Tables 1 and 2, were validated by real-time PCR on triplicate samples.

PCR-based analysis of transcript levels. For reverse transcription and semiquantitative PCR analysis, total RNA was subject to purification with an RNeasy RNA purification kit with DNase I treatment (Qiagen, Valencia, CA), and 5 μ g were used for first-strand cDNA synthesis with SuperScript II RNase H-RT (Invitrogen) and an oligo(dT)-22 primer. For real-time PCR assessments, first-strand cDNA was synthesized as described above using 3 μ g of DNase I-treated total RNA. Target cDNA levels were analyzed by SYBR Green-based real-time PCR in 25- μ l reactions containing 1 \times SYBR Green PCR Master Mix (Applied Biosystems, Foster City, CA), 200 nM each forward and reverse primers, and 10 or 50 ng of cDNA.

Table 1. *Genes upregulated in ScAP-23 adipogenesis*

Gene ID	Unigene	Gene Name	Symbol	Fold Increase*
M11768	Mm.4407	Complement factor D	Cfd	150,000
U37222	Mm.3969	Adiponectin	Adipoq	83,000
Z22661	Mm.182440	Apolipoprotein C-I	Apoc1	3,600
S67972	Mm.26730	Haptoglobin	Hp	1,300
L23108	Mm.18628	CD36 antigen	Cd36	760
M27796	Mm.300	Carbonic anhydrase 3	Car3	20
X14607	Mm.9537	Lipocalin 2	Lcn2	20
AF045887	Mm.301626	Angiotensinogen	Agt	15
K02109	Mm.582	Fatty acid binding protein 4 (aFABP)	Fabp4	5
M60847	Mm.1514	Lipoprotein lipase	Lpl	4

Gene ID was provided by BD Atlas Mouse 1.2 Array II (Clontech). ScAP-23, subcutaneous adipocyte precursor, cell line-23. *Values >10 were rounded to 2 significant digits and are representative of repeat analyses of real-time PCR-based transcript expression.

Real-time PCR was conducted with an ABI 7500 Real-Time PCR System. PCR was carried out over 40 cycles of 95°C for 15 s, 60°C for 30 s, and 72°C for 40 s, with an initial cycle of 50°C for 2 min and 95°C for 10 min to activate AmpliTaq Gold DNA polymerase; a dissociation curve was generated over the range of 60–95°C. Expression of each gene was normalized against Gapdh transcript level. In all cases, the same amount of input RNA/cDNA was used in side-by-side comparisons, and the Gapdh level for these samples differed by two or fewer cycles. The cycle threshold (Ct) value was generated using ABI Prism 7500 SDS software, version 1.2, and then exported to a Microsoft Excel spreadsheet. Fold changes were calculated and are shown as means \pm SD in triplicate. For Table 1, transcript expression level in preadipocytes was set at a value of 1; for Table 2, transcript expression in adipocytes was set at a value of 1. In cases where transcript expression was not evident after 40 PCR cycles, a value of 40 cycles was assigned to that sample to calculate the delta Ct and express fold differences. This was done for the preadipocyte value for adiponectin, angiotensinogen, and adipisin in Table 1; other such instances are noted in the respective figure legends. All primer pairs

used in semiquantitative and real-time PCR studies are presented as Supplemental Table (supplemental data are available at the online version of this article). Semiquantitative PCR gel data presented as contiguous lanes and shown as an inclusive panel arose from a single original image of one agarose gel. However, as noted in the respective figure legend, in some instances data lanes were removed or rearranged for clarity or economy of presentation.

Insulin receptor immunoprecipitation and immunoblotting. ScAP-23 adipocytes were incubated with serum-free media or serum-free media containing insulin for 16 h, followed by a 5-min incubation with 100 nM insulin. Cells were harvested in lysis buffer containing 50 mM Tris·HCl, pH 7.4, 1% NP-40, 150 mM NaCl, 1 mM EDTA, 1 mM PMSF, 200 μ M Na₃VO₄, 1 mM NaF, 1% protease inhibitor cocktail (cat. no. P8340, Sigma-Aldrich), 1% phosphatase inhibitor cocktail (cat. no. P5726, Sigma-Aldrich), 1 μ g/ml aprotinin, 1 μ g/ml leupeptin, and 1 μ g/ml pepstatin for 45 min at 4°C, after which fat cake and insoluble material were removed. For immunoprecipitation, cell lysates were incubated overnight with mouse monoclonal antibody to insulin receptor- β (IR- β) [Santa Cruz Biotechnology (C-19), Santa

Table 2. *Genes downregulated in ScAP-23 adipogenesis*

Gene ID	Unigene	Gene Name	Symbol	Fold Decrease*
Y07519	Mm.289824	Interleukin 1 receptor-like 1	Il1rl1	1,400
D21099	Mm.3488	Aurora kinase B	Aurkb	220
D00208	Mm.3925	S100 calcium binding protein A4	S100a4	390
M65142	Mm.172	Lysyl oxidase	Lox	360
J04467	Mm.290320	Chemokine (C-C motif) ligand 2	Ccl2	200
L01640	Mm.6839	Cyclin-dependent kinase 4	Cdk4	180
L07803	Mm.26688	Thrombospondin 2	Thbs2	140
K03235	Mm.88796	Proliferin	Pif2	120
U08020	Mm.277735	Procollagen, type I, alpha1	Coll1a1	100
M31885	Mm.444	Inhibitor of DNA binding 1	Id1	80
U58633	Mm.281367	Cell division cycle 2 homolog A	Cdc2a	75
X51396	Mm.4173	Microtubule-associated protein 1 B	Mtap1b	65
L33726	Mm.289707	Fascin homolog 1, actin bundling protein	Fscn1	60
M26071	Mm.273188	Coagulation factor III	F3	55
X12801	Mm.204969	Spectrin alpha2	Spna2	55
L07063	Mm.3894	FK506 binding protein 10	Fkbp10	50
M36830	Mm.341186	Heat shock protein 90kDa alpha class A member 1	Hsp90aa1	50
M90364	Mm.291928	Catenin (cadherin associated protein), beta1	Ctnnb1	40
X79233	Mm.142822	Ewing sarcoma breakpoint region 1	Ewsr1	40
AB017189	Mm.27943	Solute carrier family 7	Slc7a5	40
M57470*	Mm.43831	Lectin, galactose binding, soluble 1	Lgals1	30
X81584	Mm.358609	Insulin-like growth factor binding protein 6	Igfbp6	20
U76112	Mm.185453	Eukaryotic translation initiation factor 4, gamma2	Eif4g2	20
X63535	Mm.4128	AXL receptor tyrosine kinase	Axl	20
U49351	Mm.4793	Glucosidase, alpha, acid	Gaa	20
D50460	Mm.2044	Serine peptidase inhibitor, clade F, member 1	Serpinf1	5

Gene ID provided by BD Atlas Mouse 1.2 Array II (Clontech). *Values >10 are rounded to 2 significant digits and are representative of repeat analyses by real-time PCR.

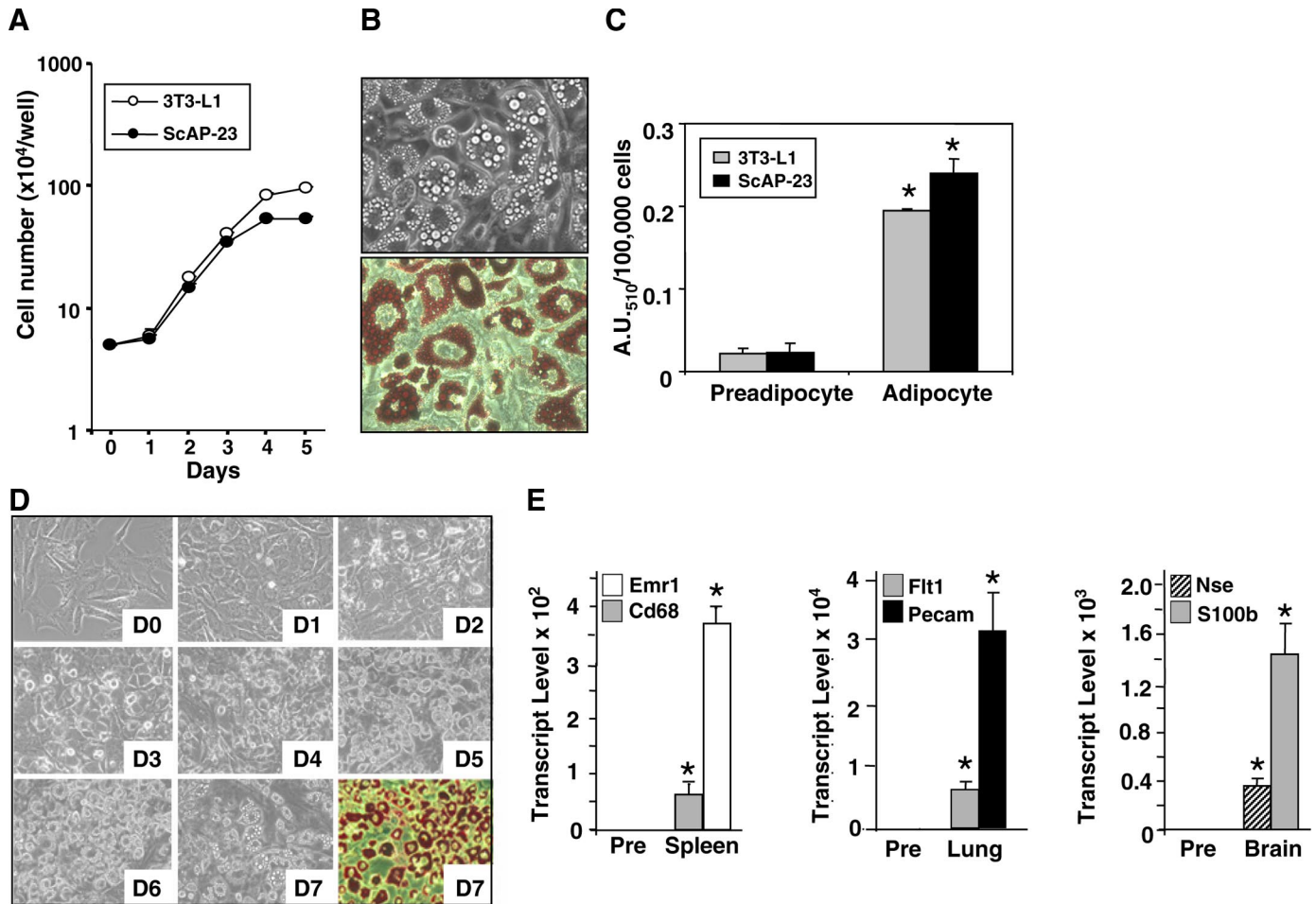


Fig. 1. Cell growth and differentiation of ScAP-23. *A*: ScAP-23 cells and 3T3-L1 cells were plated in triplicate and counted every 24 h for 5 days. Data represent means \pm SD from 3 independent experiments. *B*: ScAP-23 cells were plated and differentiated with methylisobutylxanthine (MIX), dexamethasone (Dex), insulin, and indomethacin (Indo) treatment. The morphology of differentiated ScAP-23 cells at *day 7* was observed under phase contrast (*top*), and lipid droplets were visualized by Oil Red O staining (*bottom*). *C*: ScAP-23 cells and 3T3-L1 cells were stained with Oil Red O before differentiation (Preadipocyte) and at *day 7* of differentiation (Adipocyte). Oil Red O stain was extracted with isopropanol and diluted at 1:10, and absorbance was measured at 510 nm [absorbance units (A.U.)₅₁₀]. **P* < 0.001 compared with respective preadipocyte value. *D*: ScAP-23 cells were differentiated with Dex, MIX, insulin, and Indo treatment. Phase-contrast images are of ScAP-23 cells before differentiation (D0) and after induction of differentiation (D1–D7). Oil Red O staining at *day 7* (D7) is shown at the *bottom right*. *E*: assessment of ScAP-23 preadipocytes for expression of macrophage (*left*), endothelial (*middle*), and neuronal (*right*) mRNA marker transcripts. Two marker transcripts are shown in each graph, as indicated, and the transcript level detected in ScAP-23 has been set to 1. **P* < 0.001 compared with ScAP-23 preadipocytes. For endothelial markers, ScAP-23 transcript was not detected after 40 PCR cycles. In this case, to indicate the magnitude of gene expression differences, a value of 40 cycles was assigned in calculating delta Ct. Ct, cycle threshold.

Cruz, CA] and protein A-agarose at 4°C with constant mixing. Agarose beads were washed three times with lysis buffer and boiled in Laemmli sample buffer. For immunoblotting, immunoprecipitates or whole cell lysates were resolved by 10% SDS-PAGE or by 10% NuPAGE gel (Invitrogen) and electroblotted to Immobilon-P membrane (Millipore, Bedford, MA). Following transfer, membranes were blocked in 5% nonfat milk in PBS-0.5% Tween 20 (PBS-T) for 1 h and incubated, as indicated, with antibodies to phosphotyrosine (cat. no. 4G10, Upstate, Charlottesville, VA), IR-1 β (cat. no. SC-711, Santa Cruz Biotechnology), PPAR γ (cat. no. SC-7273, Santa Cruz Biotechnology), or tubulin (cat. no. MMS-410P, Covance Research Products, Berkeley, CA). Following primary antibody incubation, membranes were washed and incubated with horseradish peroxidase-conjugated secondary antibody (Bio-Rad, Hercules, CA). All washings of Western blots were conducted in PBS-T. After the final wash, signals were detected by incubation in enhanced chemiluminescence plus reagent (GE Healthcare) and exposure to Fuji RX film. Western blot data presented as contiguous lanes and shown as an inclusive panel arose from a single original image of one Western blot.

However, as noted in the respective figure legend, in some instances data lanes were removed or rearranged for clarity or economy of presentation.

RESULTS AND DISCUSSION

Growth characteristics of ScAP-23 preadipocytes. Following \sim 70 doublings, ScAP-23 was selected as a permanent clonal preadipocyte cell line and expanded for an additional 70 doublings. ScAP-23 cells were demonstrated to express transcript for hTERT by semiquantitative PCR (data not shown). It was noted during the establishment of this cell line that while the morphology of the cells was typically fibroblastic, some individual cells within the population underwent spontaneous conversion to adipocytes. We also observed that cells began to grow poorly and appeared generally unhealthy at higher densities when cultured in media containing FCS. Substitution of calf serum for the FCS resulted in cell growth that was more

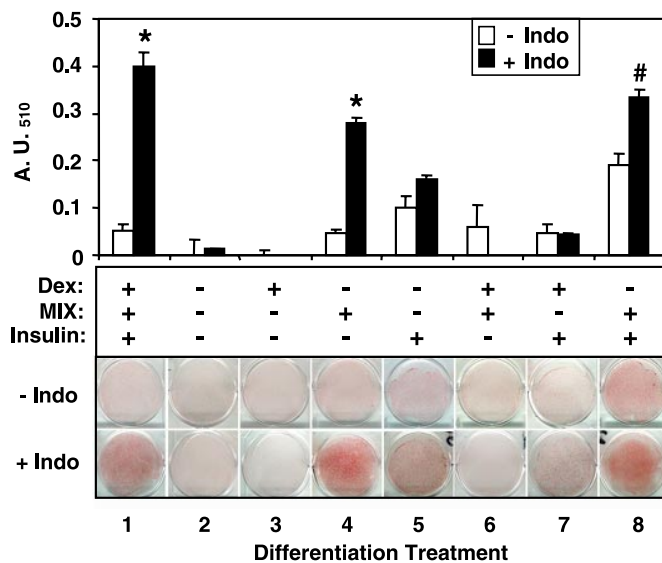


Fig. 2. Indo effect on adipogenesis of ScAP-23 cells. Cells were treated with indicated combinations of Dex, MIX, and insulin with (+) or without (-) Indo for 3 days and maintained in DMEM-10% FCS for 4 additional days. Representative Oil Red O-stained culture dishes are shown. Oil Red O stain was extracted and diluted at 1:10, and absorbance was measured at 510 nm. Bar graph indicates differentiation treatment in the presence (solid bars) or absence (open bars) of Indo. Data represent means \pm SD, analyzed by single-factor ANOVA. * P < 0.005, # P < 0.05 compared with “-Indo” treatments.

stable and uniform. To determine the growth parameters of the ScAP-23 preadipocytes and to compare their growth rate with that of 3T3-L1 cells, equal cell numbers of each were plated, and cell number was determined at daily intervals. Figure 1A indicates that ScAP-23 cells have a doubling time of 14–16 h.

Indomethacin is a key agent for the adipogenic conversion of ScAP-23 preadipocytes. While a degree of spontaneous adipocyte conversion was noted to occur sporadically during the establishment of the ScAP-23 clonal line, the utility of this new cell line to the study of adipogenesis was dependent on defining optimal conditions for full adipose conversion. We first tested the 0.5 mM MIX, 1 μ M dexamethasone, and 17 nM insulin (MDI) differentiation protocol carried out in the presence of FCS-containing media. We found that this protocol, although a standard one for adipogenic conversion of 3T3-L1 preadipocytes, was not effective in propelling ScAP-23 preadipocytes to an adipocyte phenotype. The literature indicated the occasional use of indomethacin, a nonsteroidal anti-inflammatory drug that can bind and activate PPAR γ , for inducing adipogenesis in some types of preadipocytes (69). Although not reported in regard to adipogenesis, indomethacin has also been reported to induce growth arrest in a number of cell lines (6, 16, 25, 92). We therefore ascertained the affects of supplementing the MDI treatment with indomethacin (MDI+Indo), in the presence of FCS-containing media. Figure 1B shows that the use of the MDI+Indo adipogenic cocktail resulted in >90% adipocyte conversion of ScAP-23 preadipocytes, as assessed by cell morphology (Fig. 1B), lipid droplet accumulation, and Oil Red O staining of intracellular lipid (Fig. 1, B–D). Thus, in contrast to the differentiation regimen for 3T3-L1 preadipocytes, we find that effective adipose differentiation of ScAP-23 preadipocytes depends on inclusion of

indomethacin in the adipogenic cocktail. To facilitate uniform differentiation, we do not typically treat less-than-confluent ScAP-23 cells for adipogenic induction; however, we have observed that individual ScAP-23 cells have the ability to undergo either spontaneous or induced adipogenesis without requiring confluence (data not shown). We also note here that the protocol we have established for ScAP-23 cells involves treatment with adipogenic inducing agents when cells just attain confluence, as postconfluent ScAP-23 cells appeared unhealthy. This differs from the standard 3T3-L1 differentiation protocol, wherein preadipocytes are treated with adipogenic inducing agents at 2 days postconfluence (101).

We next documented the morphological alterations in ScAP-23 cells over an 8-day period from the preadipocyte state (*day 0*) through 7 days postinduction with the MDI+Indo protocol (Fig. 1D). A few cells that contained lipid droplets appeared by 3 days postinduction, and by *day 4*, a much greater percentage of cells contained small lipid droplets; these in-

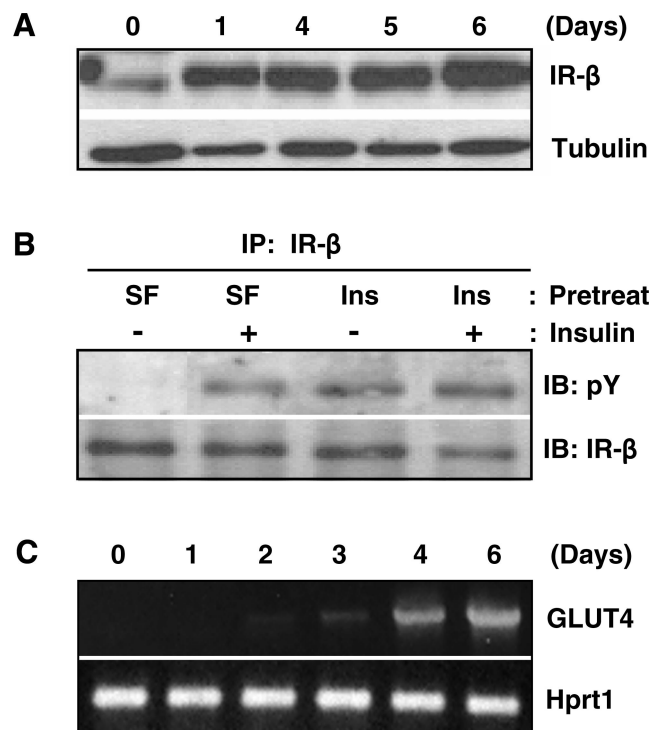


Fig. 3. Molecular aspects of insulin signaling in ScAP-23 cells. A: differentiation-dependent insulin receptor- β (IR- β) expression in ScAP-23 cells. Protein was harvested from ScAP-23 cells before differentiation (*day 0*) and at indicated days postinduction of differentiation. Western blot analysis was performed using IR- β antibody with tubulin shown as a control. B: IR- β phosphorylation by insulin in ScAP-23 cells. Differentiated ScAP-23 cells were incubated in serum-free medium (SF) or insulin-containing (Ins) medium for 16 h and then stimulated with insulin for 5 min. Protein lysates were subjected to immunoprecipitation (IP) with IR- β antibody followed by immunoblotting (IB) with phosphotyrosine (pY) antibody or IR- β antibody. C: GLUT4 expression during ScAP-23 adipogenesis. RNA was harvested from ScAP-23 cells before differentiation (*day 0*) and on indicated days postinduction of differentiation. RT-PCR was performed using a primer set specific for GLUT4. Hypoxanthine guanine phosphoribosyl transferase-1 (Hprt1) was used as a control. As described in MATERIALS AND METHODS, quantitation of GLUT4 transcript expression was also determined by real-time PCR. For A, B, and C, data presented in each horizontal panel were obtained from one single original image. For A and B, data lanes were removed or rearranged for clarity or economy of presentation.

creased in size through the last time point examined, *day 7*. Also shown in Fig. 1D, *bottom right*, are ScAP-23 adipocytes at *day 7* postinduction; these cells have been stained for intracellular lipid with Oil Red O. Quantitation of the Oil Red O staining for ScAP-23 cells and 3T3-L1 cells indicates that ScAP-23 adipocytes accumulate a level of lipid that is of a similar magnitude as 3T3-L1 adipocytes (Fig. 1C). We also assessed whether ScAP-23 cells express marker transcripts for other cell lineages that would be present in adipose tissue, namely macrophage (Emr1 and Cd68), endothelial (Flt1 and Pecam), and neuronal (Nse and S100b), with samples subjected to 40 cycles of real-time PCR. Expression of these cell type-

specific marker transcripts was nearly undetectable in ScAP-23 preadipocytes in regard to macrophage and neuronal markers and undetectable for endothelial markers (Fig. 1E).

Since we had observed that addition of indomethacin to the MDI cocktail resulted in a high level of adipose conversion, we next wished to ascertain the contribution(s) of each of these four proadipogenic agents to the induction of ScAP-23 adipogenesis. We altered the composition of the differentiation treatments by using combinations of dexamethasone, MIX, insulin, and/or indomethacin and assayed for adipocyte conversion with Oil Red O staining, as shown in Fig. 2. Of the four agents tested, inclusion of indomethacin was necessary for effective ScAP-23 adipogenesis (*treatment 1*); however, treatment with indomethacin alone was not sufficient to promote adipose conversion of ScAP-23 preadipocytes (*treatment 2*). When indomethacin was added with MIX alone (*treatment 4*), or with MIX and insulin in combination (*treatment 8*), we observed a statistically significant enhancement of adipogenesis relative to that observed when these agents were used in the absence of indomethacin. From these studies, we concluded that the optimal protocol for adipogenic conversion of ScAP-23 cells is MDI+Indo.

Molecular aspects of insulin signaling in ScAP-23 adipocytes. An exhaustive physiological and transcriptional characterization of this new in vitro model for adipogenesis can be explored in future studies; however, we thought it was important at this stage to determine whether ScAP-23 adipocytes evidenced indexes of insulin responsiveness. Western blot analysis, as shown in Fig. 3A, indicates that adipogenesis of ScAP-23 cells is accompanied by the appearance of insulin receptor- β expression, which is first noted 1 day postinduction of adipogenesis. To examine the responsiveness of the insulin signaling through the insulin receptor, we determined the insulin-mediated autophosphorylation of insulin receptor- β in ScAP-23 adipocytes. As is shown in Fig. 3B, increased insulin receptor- β phosphorylation was noted on addition of insulin to ScAP-23 adipocytes under serum-free culture conditions. Last, Fig. 3C shows the semiquantitative RT-PCR assessment indicating that the transcript level for GLUT4, the major insulin-responsive glucose transporter in adipocytes, is upregulated ~ 60 -fold ($P < 0.001$) in mature *day 6* adipocytes compared with preadipocytes; it is first detected at 2 days postinduction and dramatically increased by *day 4*.

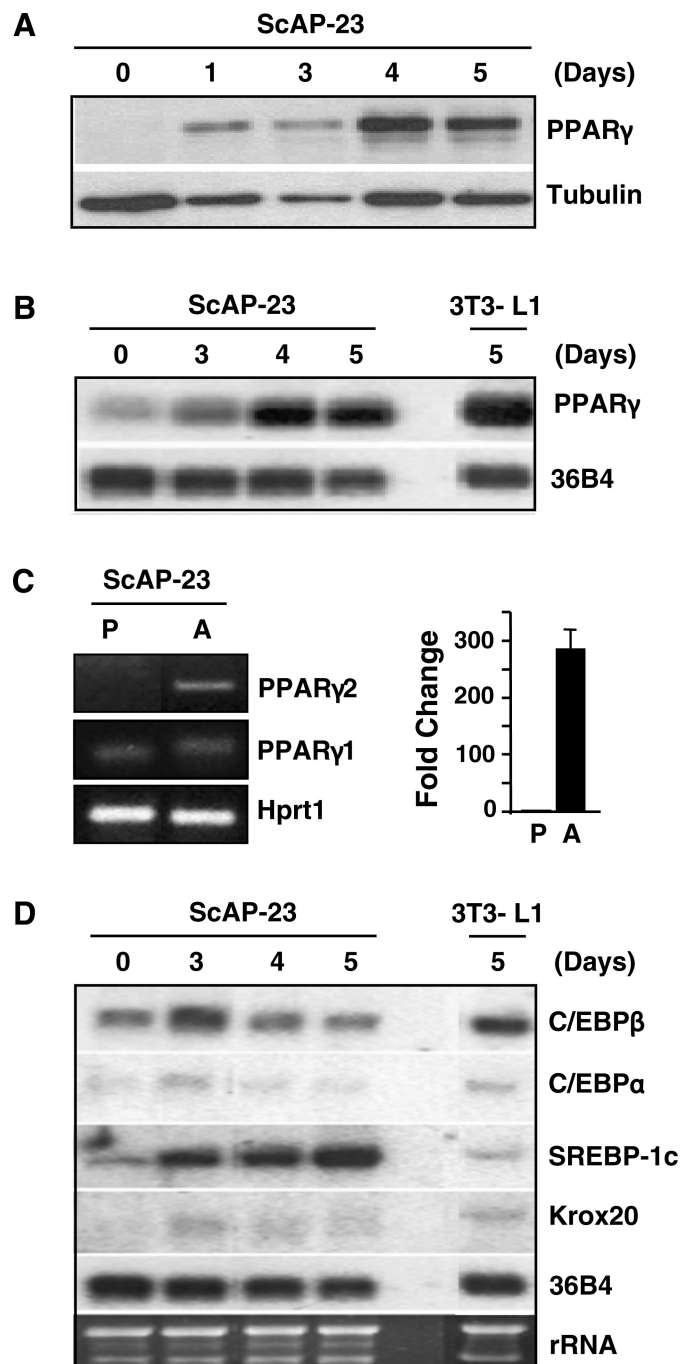


Fig. 4. Expression of peroxisome proliferator-activated receptor- γ (PPAR γ) and other transcription factors during ScAP-23 adipogenesis. *A*: expression of PPAR γ protein in ScAP-23 adipocytes. Protein was harvested from ScAP-23 cells before differentiation (*day 0*) and at indicated time points after induction of differentiation. Western blot analysis was performed using monoclonal PPAR γ antibody with tubulin as a loading control. *B*: expression of PPAR γ transcript. RNA was harvested from ScAP-23 cells at the indicated time points postinduction of differentiation or from 3T3-L1 adipocytes and analyzed by Northern blot using PPAR γ probe. 36B4 was used as a gel loading control. *C*: PPAR γ 2 expression in ScAP-23 adipocytes. ScAP-23 cells were harvested before differentiation (P) or after adipogenic conversion (A). RT-PCR was performed using specific primer sets for PPAR γ 1 and PPAR γ 2. Hprt1 was used as a control (*left*). Real-time PCR analysis was conducted for PPAR γ 2 (*right*). Preadipocyte level of PPAR γ transcript was set at 1. *D*: 5 μ g of total RNA from ScAP-23 cells at the indicated days postinduction of differentiation or from 3T3-L1 adipocytes were analyzed by Northern blot using C/EBP β , C/EBP α , SREBP-1c, and Krox20 probes. 36B4 expression and ethidium bromide (EtBr) staining of rRNA were used as gel loading control. For *A*, *B*, *C*, and *D*, data presented in each horizontal panel were obtained from one single original image. For *B–D* data lanes were removed or rearranged for clarity or economy of presentation.

Expression of key adipogenic transcription factors in ScAP-23 adipogenesis. We next addressed the expression of the master adipogenic transcription factor PPAR γ (82) during adipose conversion of ScAP-23 preadipocytes. Figure 4A shows a Western blot analysis of the time course of upregulation of PPAR γ protein level and indicates that increased PPAR γ protein expression is noted by 1 day postinduction of ScAP-23 adipogenesis and is maximally expressed at *days 4* and *5*. To examine the PPAR γ transcript level, we used Northern blot analysis (Fig. 4B) and PCR (Fig. 4C). The temporal increase in PPAR γ transcript is maximal at *days 4* and *5*, as was found for PPAR γ protein. In addition, the level of PPAR γ transcript is similar in ScAP-23 adipocytes and 3T3-L1 adipocytes. It is known that two isoforms exist for PPAR γ , with PPAR γ 1 evidencing a more general expression pattern and PPAR γ 2 being the adipocyte-specific form. To distinguish between expression of PPAR γ 1 and PPAR γ 2 in ScAP-23 cells, we conducted semiquantitative RT-PCR analysis. As Fig. 4C, *left*, demonstrates, it is only the level of the adipocyte-specific PPAR γ 2 form that increases during ScAP-23 adipocyte differentiation, and real-time PCR (Fig. 4C, *right*) indicates an \sim 280-fold upregulation ($P < 0.001$). To begin to address the expression of other transcription factors known to play important roles in adipogenesis, we used Northern blot analysis (Fig. 4D) to assess the level of C/EBP family members (112) and sterol response element binding protein-1c (SREBP-1c) (57, 90) as well as Krox20/Egr2, a gene newly identified to play a role in early events in adipocyte differentiation of 3T3-L1 cells (17). For C/EBP α , we observe an upregulation of approximately eightfold ($P < 0.01$) at *day 3*. This is consistent with the temporal early upregulation of this gene in the 3T3-L1 model that occurs proximal to treatment with adipogenic inducers (112). However, while the Northern blot analysis appears to show upregulation of C/EBP β at *day 3*, this was not validated by real-time PCR (data not shown). C/EBP β is critical to early 3T3-L1 adipogenesis (71); its role in ScAP-23 adipogenesis can be more precisely addressed in future studies. Krox20/Egr2 transcript is present at detectable levels and increases \sim 25-fold ($P < 0.01$) at *day 3* of ScAP-23 adipogenesis. SREBP-1c transcript increases \sim 4-fold at *day 3* ($P < 0.01$) and \sim 10-fold at *day 5* ($P < 0.01$). This figure also demonstrates that the levels of transcripts for C/EBP α , C/EBP β , and Krox20/Egr2 are of a similar magnitude in ScAP-23 and 3T3-L1 adipocytes; however, the level of SREBP-1c transcript, a key player in the transcriptional regulation of genes functioning in lipid homeostasis (90), appears higher in ScAP-23 adipocytes than in 3T3-L1 adipocytes. Future studies can more precisely dissect the regulation of expression, as well as the function, of adipogenic transcription factors in ScAP-23 adipogenesis and attempt to identify new transcriptional regulators of adipogenesis in this model.

Expression of adipocyte and preadipocyte marker genes in ScAP-23 adipocytes. As an initial molecular assessment of the molecular phenotype of ScAP-23 cells, we conducted Northern blot analysis on ScAP-23 adipocytes using several standard mRNA markers for mature adipocytes, namely, stearoyl-coenzyme A desaturase-1 (SCD1), adipocyte fatty acid binding protein (aFABP), lipoprotein lipase, glycerol-3-phosphate dehydrogenase, and fatty acid synthase. The Northern blot analysis in Fig. 5A indicates that SCD1 and aFABP transcripts are upregulated during ScAP-23 adipocytes. Real-time PCR indi-

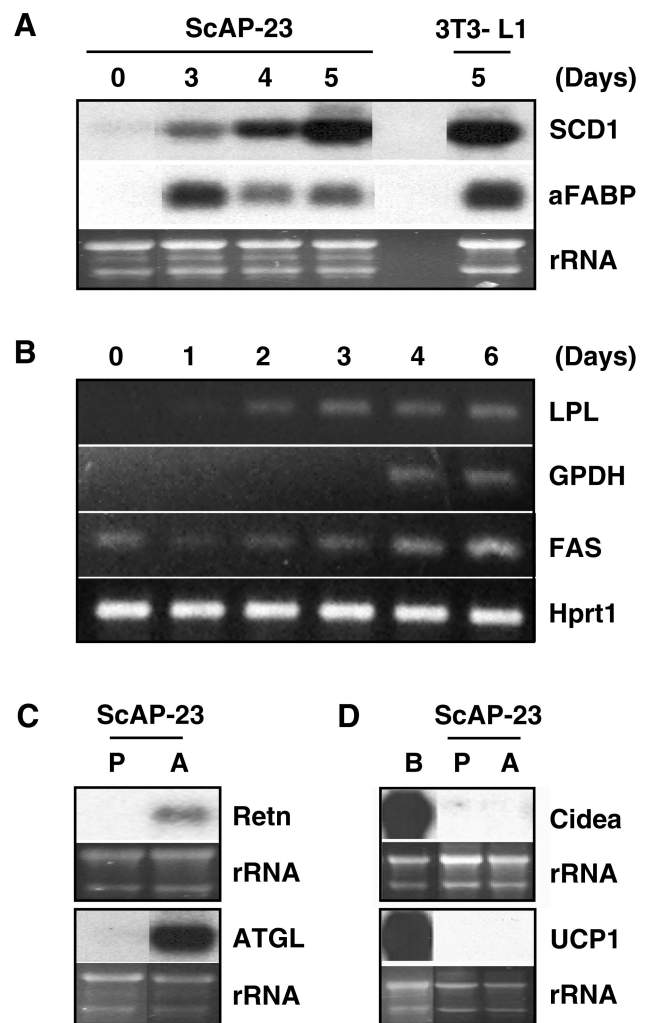


Fig. 5. Expression of adipogenesis markers. *A*: RNA was harvested from ScAP-23 cells before differentiation (*day 0*) and at indicated time points of postinduction or from 3T3-L1 adipocytes and analyzed by Northern blot using mouse SCD1 and aFABP cDNA probes. EtBr staining of rRNA was used as a gel loading control. *B*: RNA was harvested before induction of adipogenesis (*day 0*) and at indicated time points from ScAP-23 cells, and RT-PCR was performed using specific primer sets for lipoprotein lipase (LPL), glycerol-3-phosphate dehydrogenase (GPDH), and fatty acid synthase (FAS). Hprt1 was used as a control. *C*: RNA was harvested from ScAP-23 cell preadipocytes (P) or adipocytes (A) and subject to Northern blot analysis for resistin (Retn) and adipose triglyceride lipase (ATGL) transcript level. *D*: lack of brown adipocyte marker transcript expression in ScAP-23 cells. ScAP-23 cells were harvested from preadipocytes (P) and adipocytes (A), and Northern blot analysis was performed with Cidea and uncoupling protein-1 (UCP1) probes. Brown adipose tissue (B) was used as a positive control. EtBr staining of rRNA was used as a gel loading control. For *A*, *B*, *C*, and *D*, data presented in each horizontal panel were obtained from one single original image. For *A*, *C*, and *D*, data lanes were removed or rearranged for clarity or economy of presentation.

cated that SCD1 increased \sim 20-fold ($P < 0.001$) during conversion of ScAP-23 preadipocytes to *day 5* adipocytes, and a 5-fold ($P < 0.001$) increase in aFABP transcript level was found. The relatively modest degree of upregulation of aFABP was not due to lack of robust transcript expression in adipocytes but rather to the expression of easily detectable levels of aFABP transcript in ScAP-23 preadipocytes. Although this is not readily apparent on the Northern blot in Fig. 5A, it was evident in real-time PCR-based assessment (data not shown).

A similar observation had been reported by Friedman and colleagues (94) when they reported on inconsistencies between adipogenesis in vitro and in vivo for aFABP transcript expression. Although they noted that the presence of aFABP was 2.7-fold higher in wild-type mature adipocytes in vivo than in preadipocytes, it was still expressed at high levels in preadipocytes in vivo (94). This is in line with our findings regarding aFABP expression in ScAP-23 adipogenesis. This might suggest that, compared with 3T3-L1 preadipocytes, ScAP-23 preadipocytes may be more reflective of the in vivo state of preadipocyte/adipocyte gene expression.

Semiquantitative PCR assessment (Fig. 5B) and real-time PCR analysis indicates that ScAP-23 adipogenesis is accompanied by an increase in lipoprotein lipase transcript (~4-fold, $P < 0.001$) as well as that of glycerol-3-phosphate dehydrogenase and fatty acid synthase (~7-fold, $P < 0.001$). We also detected upregulation of the adipocyte-specific adipokine resistin (1,100-fold, $P < 0.001$) and the newly discovered lipase adipose triglyceride lipase (ATGL) (25-fold, $P < 0.001$) in ScAP-23 adipogenesis (Fig. 5C). A number of recent studies have indicated that cells within the WAT depot may, under certain conditions, come to resemble brown adipocytes (19, 44, 125). Even though the ScAP-23 cell line was derived from a WAT depot and morphologically resembles white adipocytes, we thought it important to examine whether ScAP-23 cells might show evidence of brown adipocyte-specific gene expression. Examination of two brown adipocyte-specific marker transcripts, Cidea and uncoupling protein-1 (UCP1), indicates that, while each is readily detected in brown adipose tissue, neither is found in ScAP-23 preadipocytes or adipocytes (Fig. 5D), consistent with a white adipocyte lineage for ScAP-23 cells.

To assess gene expression at the preadipocyte stage, we chose several genes known to decrease during 3T3-L1 adipogenesis and used Northern blot analysis to assess their expression levels in ScAP-23 and 3T3-L1 preadipocytes and adipocytes. We first analyzed expression of *pref-1*. *Pref-1* is an EGF-repeat transmembrane protein that is cleaved to release a soluble inhibitor of adipogenesis, and the *pref-1* gene product is abundant in 3T3-L1 preadipocytes and dramatically decreases on their adipocyte conversion (91). The Northern blot in Fig. 6A and the real-time PCR analysis in Fig. 6B reveal that ScAP-23 adipogenesis is accompanied by a decrease in *pref-1* level to ~6% ($P < 0.001$) of that present in ScAP-23 preadipocytes. In contrast to the relatively low level of *pref-1* transcript level in ScAP-23 preadipocytes, 3T3-L1 preadipocytes express markedly higher levels of *pref-1* transcript (~340-fold higher than ScAP-23 preadipocytes, $P < 0.001$) (Fig. 6D). This is reduced by 90% ($P < 0.001$) on their adipocyte conversion, as expected (91) (Fig. 6B).

We also compared *pref-1* transcript level in ScAP-23 preadipocytes with the level of *pref-1* transcript in the preadipocyte-containing stromal-vascular fraction and the adipocyte fraction of adipose tissue. Figure 6C shows effective fractionation of adipose tissue into the stromal-vascular fraction and adipocyte fractions, as assessed by expression of the adipocyte marker resistin and the stromal marker collagen1A1. Analyses of *pref-1* transcript in these fractions, as well as *pref-1* transcript levels in ScAP-23 and 3T3-L1 preadipocytes, are shown in Fig. 6D. We show that 3T3-L1 preadipocytes express ~50 times the level of *pref-1* transcript compared with the adipose

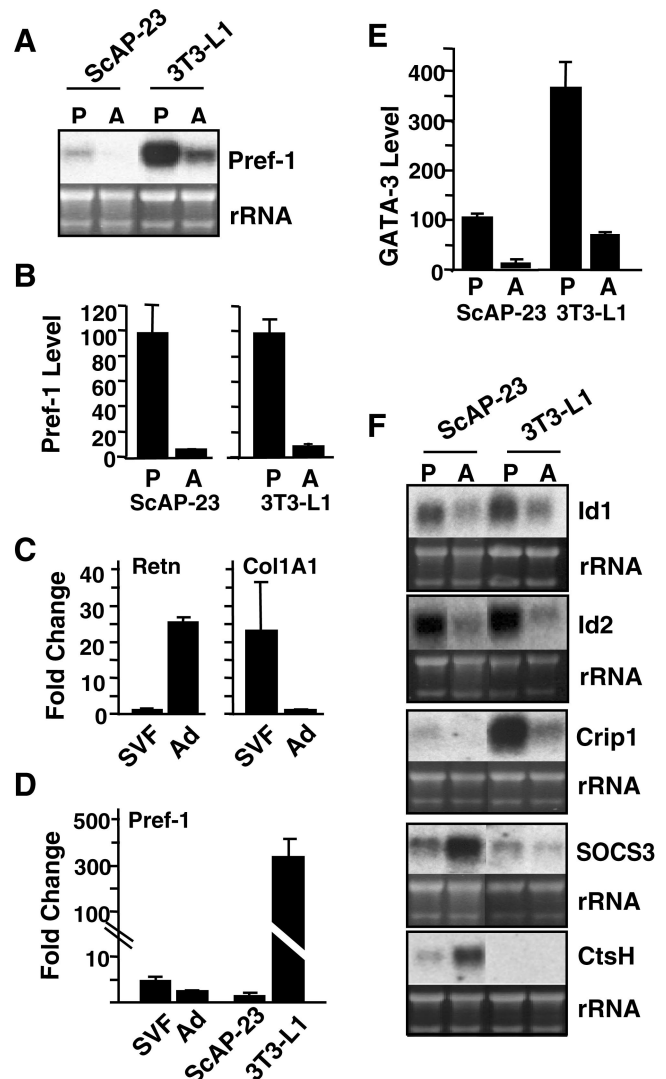


Fig. 6. Distinct gene expression in adipogenesis of ScAP-23 cells and 3T3-L1 cells. RNA was harvested from ScAP-23 and 3T3-L1 preadipocytes (P) and adipocytes (A) or the adipocyte (Ad) or stromal-vascular fraction (SVF) of murine subcutaneous white adipose tissue (WAT). A: Northern blot analysis was performed using *pref-1* probe with EtBr staining of rRNA shown as a gel loading control. B: assessment by real-time PCR of *pref-1* transcript level in ScAP-23 and 3T3-L1 preadipocytes and adipocytes. Preadipocyte level of *pref-1* transcript was set to 100. C: effective fractionation of WAT into SVF and Ad cell populations as assessed by relative transcript expression for resistin (*Retn*) and collagen1A1 (*Col1A1*). The SVF value was set to 1 for the *Retn* panel, and the Ad value was set to 1 for the *Col1A1* panel. D: comparison of *pref-1* transcript level in SVF, Ad, ScAP-23 preadipocytes and 3T3-L1 preadipocytes by real-time PCR. The level of *pref-1* transcript in ScAP-23 preadipocytes was set to 1. E: assessment of downregulation of GATA-3 transcript during ScAP-23 and 3T3-L1 adipogenesis. The level in ScAP-23 preadipocytes was set to 100. F: Northern blot analysis was performed using indicated probes with EtBr staining of rRNA shown as a gel loading control. For B–E, P values are stated in RESULTS AND DISCUSSION. For A and F, data presented as inclusive panels were obtained from one single original image of a gel or autoradiogram. Some lanes of the original images have been removed and/or rearranged for clarity or economy of presentation.

tissue stromal-vascular fraction. In contrast, the expression of *pref-1* in ScAP-23 cells is present at levels that are within sevenfold of the level found in the stromal-vascular cell population. Although difficult to precisely determine in vivo, it has been estimated that 15–50% of cells in the stromal-vascular

fraction of adipose tissue are preadipocytes (61, 106). If 50% of the stromal-vascular fraction cells represent preadipocytes, we would expect a twofold enrichment of *pref-1* transcript in ScAP-23 preadipocytes over the level found in the stromal-vascular fraction. Thus the level of *pref-1* transcript in ScAP-23 preadipocytes is somewhat less than predicted. Nevertheless, we conclude from this data that the level of *pref-1* transcript in ScAP-23 preadipocytes is more in line with its expression in vivo than with the high degree of enrichment for *pref-1* transcript found in 3T3-L1 preadipocytes, which are of embryonic origin. Microarray data generated by Friedman and colleagues (94) have revealed distinct transcriptional profiles of adipogenesis in vivo and in vitro. Similar to our data herein, they reported that *pref-1* was expressed poorly in vivo but highly enriched in 3T3-L1 preadipocytes. Future studies can further address the ability of ScAP-23 preadipocytes to effectively recapitulate aspects of in vivo preadipocytes and in vivo adipogenesis. Additional preadipocyte gene assessment in ScAP-23 adipogenesis revealed that GATA-3, a transcription factor with a key role in adipogenic conversion (108) and which is known to be expressed in 3T3-L1 preadipocytes, is present at a similar magnitude of expression in 3T3-L1 and ScAP-23 preadipocytes (~3.5-fold higher in 3T3-L1, $P < 0.001$). It is similarly downregulated on adipogenic conversion of both cell lines with a 90 and 85% reduction in ScAP-23 and 3T3-L1 adipogenesis, respectively ($P < 0.001$) (Fig. 6E). Northern blot analysis of transcript levels of the inhibitor of DNA binding helix-loop-helix factors Id1 and Id2 indicates that these transcripts are expressed at similar levels in ScAP-23 and 3T3-L1 cells and are markedly downregulated in both on adipose conversion (Fig. 6F), as has been previously demonstrated for in vitro adipogenesis (75).

In addition to variation in transcript level for ScAP-23 and 3T3-L1 cells with regard to SREBP-1c and *pref-1*, during our studies we also found evidence of further transcriptional distinctions between 3T3-L1 and ScAP-23 with regard to the level of *Crip1*, *SOCS3*, and *cathepsin H* transcripts (Fig. 6F). *Crip1* shows enriched transcript expression in 3T3-L1 preadipocytes (~40-fold increase vs. ScAP-23 preadipocytes, $P < 0.001$) and is downregulated on their adipose conversion. *Crip1* encodes a 77-amino acid cysteine-rich intestinal protein with a LIM motif; studies in transgenic mice revealed that overexpression of *Crip1* leads to an imbalance in cytokine patterns, suggesting a role in immune system function (65). To our knowledge, *Crip1* has not been previously addressed in adipogenesis. Two genes that show enriched expression in ScAP-23 are *SOCS3* and *cathepsin H*. Endogenous *SOCS3* expression in adipocytes is proposed to be a key determinant of basal insulin signaling and to be an important molecular mediator of cytokine-induced insulin resistance in adipocytes (89). Members of the *cathepsin* serine protease protein family have also come to light recently in adipocyte and adipose tissue function and obesity (97); however, *cathepsin H* has not yet been addressed in this regard. While it is possible that, to some degree, the differential gene expression found between ScAP-23 and 3T3-L1 adipocytes might stem from differences in their respective adipogenic conversion protocols, it is also reasonable to speculate that the genes most central to the function of white adipocytes would likely be similarly expressed and regulated in both cell lines. On the other hand, distinctions between ScAP-23 and 3T3-L1 preadipocytes and/or adipocytes will likely point to genes

whose function may not be essential to the most fundamental nature of adipocytes, for example triglyceride synthesis and turnover. These uniquely expressed genes might reflect, with regard to ScAP-23 cells, aspects of the molecular nature of preadipocytes and adipocytes derived from WAT. Future studies can further delineate similarities and distinctions of these two in vitro models of adipogenesis.

Assessment of capacity of ScAP-23 preadipocytes for multilineage differentiation. Multilineage differentiation of human and rodent adipose tissue-derived cells to mesenchymal derivatives or other cell lineages has been described. This is attributed to a mesenchymal or other stem cell population present in adipose tissue (36, 41, 70, 126). The shared mesenchymal lineage of adipocytes with that of chondrocytes, myocytes, and osteocytes has also been demonstrated in studies of multilineage differentiation of the CH310-T1/2 mesenchymal cell line (103) and of bone marrow-derived mesenchymal primary cells and cell lines (24, 80). As a first step in assessing the potential of ScAP-23 preadipocytes to differentiate to lineages other than adipocyte, we cultured them under conditions previously reported to promote neurogenic, myogenic, osteogenic, or chondrogenic differentiation of adipose tissue stromal stem cells. One of each of the two protocols tested for neurogenic (70), myogenic (126), or osteogenic (70) differentiation proved toxic to the cells, as did the protocol we tested for chondrogenesis (41), and as such was not subject to further analysis. We were able, however, to identify treatment protocols from the literature during which ScAP-23 cells remained viable and appeared healthy for a limited time: 3 days for neurogenesis (86) and osteogenesis (124) and 6 days for myogenesis (70). None of the tested differentiation induction treatments led to changes in cellular morphology, with the exception of a very transient morphological alteration in the several hours following application of neuronal induction conditions (data not shown). After this period, ScAP-23 cells reverted to their typical fibroblastic appearance.

We used real-time PCR to examine transcript expression of ScAP-23 cells for the expression of lineage marker genes before and during/following multilineage differentiation induction. These were neuron-specific enolase, *S100b*, and *tubulin- β 3* for neurogenesis; *myoD* and *myogenin* for myogenesis; and *runx2* and *Bglap/osteocalcin* for osteogenesis. A tissue sample enriched for these respective cell types (brain, muscle, and bone) was utilized as a positive control for lineage marker transcript expression. These data are shown in Fig. 7. With regard to neuronal markers (Fig. 7A), *S100b* and *tubulin- β 3* decreased at *days 1* and *3* postinduction ($P < 0.001$) rather than increased, as would be indicative of differentiation to a neuronal phenotype. *Nse* increased ~5-fold at *day 1* and ~8-fold at *day 3* ($P < 0.001$); however, this is ~25-fold less than the level of *Nse* transcript found in brain. Assessment at later time points was not possible because of the toxicity of culture conditions. After 40 cycles of real-time PCR, myogenic marker transcripts remained undetectable in ScAP-23 preadipocytes as well as at *days 3* and *6* of the myogenic induction protocol (Fig. 7B). An ~3-fold increase ($P < 0.05$) in *Runx2* transcript was found at *day 3* of osteogenic induction, and a 23-fold ($P < 0.001$) increase for *Bglap/osteocalcin* (Fig. 7C). However, the level of these bone markers in ScAP-23 cells is markedly less than that found in bone tissue. It is possible that by testing a wider range of differentiation conditions and/or

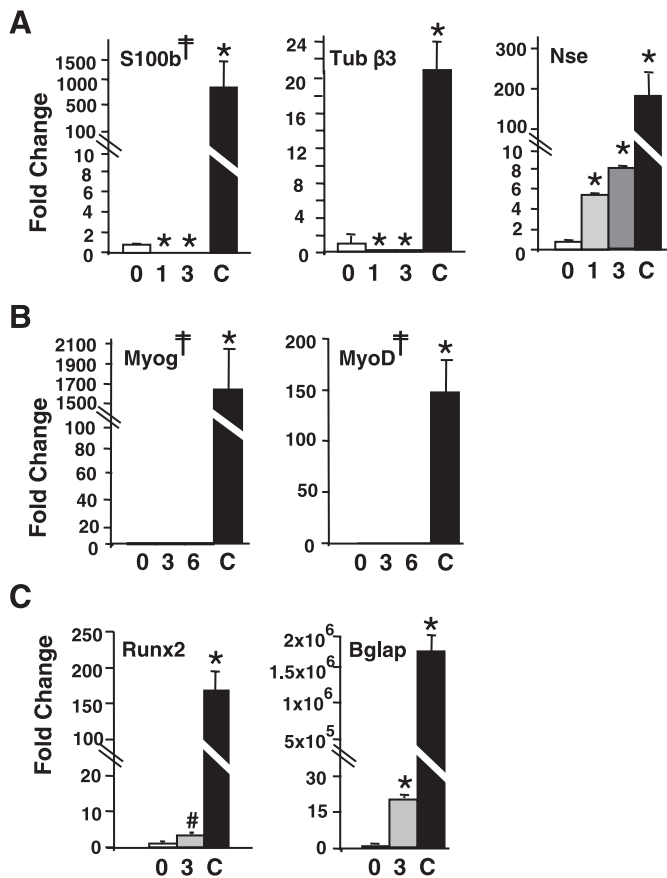


Fig. 7. Assessment of multilineage differentiation capacity of ScAP-23 preadipocytes. Real-time PCR analysis was carried out for marker transcripts indicative of neurogenic (A), myogenic (B), or osteogenic (C) differentiation. Nos. on the x-axis indicate day of treatment, with ScAP-23 preadipocytes indicated as *day 0*. The “broken” y-axes and bars indicate discontinuities of values as shown for S100b, Nse, Myog, MyoD, Runx2, and Bglap transcript levels. * $P < 0.001$, # $P < 0.05$ compared with ScAP-23 preadipocytes. For Myog and MyoD markers, ‡ indicates that transcript was not detected in ScAP-23 *day 0*, *day 3*, or *day 6* samples after 40 PCR cycles. For S100b, † indicates transcript was not detected for *day 1* and *day 3* ScAP-23 samples. In these cases, to indicate the magnitude of gene expression differences, a value of 40 cycles was assigned in calculating delta Ct. Positive controls for PCR reactions are represented by the “C” and indicate brain tissue RNA for A, muscle tissue RNA for B, and bone tissue RNA for C. Values were normalized to Gapdh expression, and the transcript expression level in *day 0* preadipocytes was set at 1. Fold changes were calculated and are shown as means \pm SD in triplicate. * $P < 0.001$, # $P < 0.05$ compared with ScAP-23 preadipocytes.

reducing the toxicity of the treatments, we might be able to formulate culture conditions for enhanced conversion of ScAP-23 cells to lineages other than adipocyte. We may also be able to force lineage differentiation via ectopic expression of various lineage-specific master regulatory transcription factors. With the caveat that our *in vitro* studies to date are limited in scope, they nonetheless support that ScAP-23 cells are of a preadipocyte/adipocyte lineage.

DNA filter array analysis of ScAP-23 adipogenesis. Our functional and gene expression assessments of ScAP-23 cells herein indicate that ScAP-23 adipocytes reflect multiple important aspects of adipocyte biology. To identify additional genes that are regulated in ScAP-23 adipogenesis, we conducted differential screening of commercial DNA nylon filter arrays with reverse-transcribed probes from ScAP-23 preadipocytes and adipocytes.

This array of 1,176 murine genes was chosen based on the high representation of metabolism-related genes. We identified 10 genes upregulated during ScAP-23 adipogenesis. Each of these genes was validated via real-time PCR, and their fold increases ($P < 0.001$) are noted in Table 1. These genes include a number of adipocyte-expressed and/or adipocyte-specific genes that have been well studied in 3T3-L1 and other models of *in vitro* and/or *in vivo* adipocytes. These are CD36 antigen (4, 31), haptoglobin (53), adiponectin (50), lipoprotein lipase (122), fatty acid binding protein-4/aFABP (7, 95), angiotensinogen (88), and complement factor D/adipsin (20). While not well studied in adipocytes, lipocalin-2 has been previously reported as induced in the 3T3-L1 model (53). Apolipoprotein C1 and carbonic anhydrase-3, while not previously described as regulated during *in vitro* adipogenesis, have been implicated in WAT function (8, 54, 113).

A large number of genes that define the adipocyte phenotype have been described, and many of these are closely linked to the physiological role of the adipocyte in lipid metabolism and whole body energy balance (82, 83, 94). In contrast to the ease in which one can identify adipocytes in the *in vitro* and *in vivo* setting, the phenotypic and molecular definition of preadipocytes remains unclear, and the study of preadipocytes is severely limited by the present lack of robust markers. A multitude of genes expressed in 3T3-L1 cells and downregulated during their adipose conversion have been reported in microarray studies over the past few years (83, 94). However, only a few of these have been further validated or characterized as preadipocyte marker genes and/or studied with regard to their function in adipocyte conversion (75, 84, 91, 108). We identified 26 genes enriched in ScAP-23 preadipocytes vs. ScAP-23 adipocytes. Transcript downregulation for each of these genes was confirmed by real-time PCR, and fold decreases were determined ($P < 0.001$) (these are listed in Table 2). We reasoned that with this new preadipocyte cell line, we might be able to begin to better identify that group of genes that is most fundamental to the preadipocyte stage. Genes that evidenced a common pattern of downregulation in two independent models of adipogenesis, namely ScAP-23 and 3T3-L1, may point to gene expression patterns important for the preadipocyte phenotype. To identify such genes, we hybridized the same nylon filter array set used to analyze ScAP-23 gene expression, with probes derived from 3T3-L1 preadipocytes and 3T3-L1 adipocytes. We chose 14 genes that appeared to be downregulated in both ScAP-23 and 3T3-L1 adipogenesis for semiquantitative PCR assessment of transcript levels. These genes represent various categories of protein function including cell cycle-related genes, secreted factors, and signaling molecules. Figure 8A shows the differentiation-dependent downregulation of these genes in ScAP-23 adipogenesis and Fig. 8B in 3T3-L1 adipogenesis.

Of the transcripts assessed by PCR, the preadipocyte-enriched expression of two of these genes in ScAP-23 adipogenesis, namely, β -catenin (Ctnnb1) and Ccl2, would be anticipated based on their previously described expression and/or function in 3T3-L1 adipogenesis. With regard to Ctnnb1, activation of the canonical β -catenin-dependent Wnt signaling pathway inhibits adipogenesis (84). Ccl2, also known as monocyte chemoattractant protein-1 (MCP-1), is produced by adipose tissue and is involved in the recruitment of monocytes to sites of inflammation and in obesity (55) and also possesses

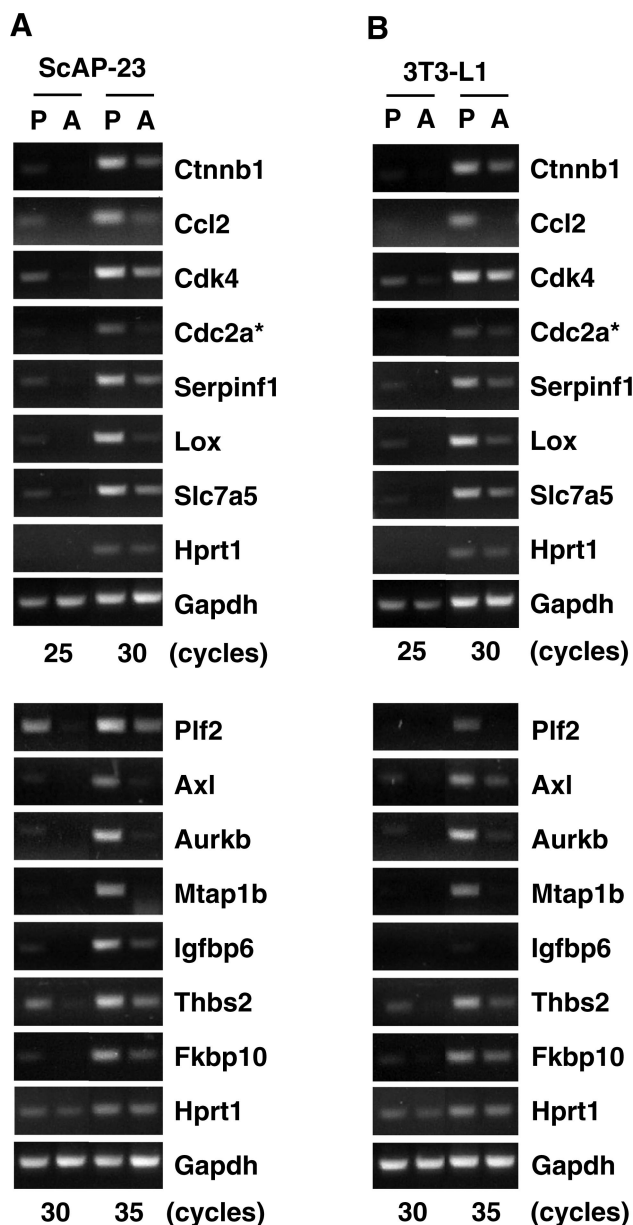


Fig. 8. Validation of gene expression in ScAP-23 and 3T3-L1 adipogenesis by semiquantitative PCR. cDNA was generated from ScAP-23 preadipocytes (P) and adipocytes (A, panel A) or from 3T3-L1 preadipocytes and adipocytes (panel B). PCR products from the indicated cycle were analyzed by agarose gel electrophoresis and EtBr staining. *Amount of template is 5 times higher than for the other reactions. Hprt1 and Gapdh were used as controls. For A and B, data presented as inclusive panels were obtained from one single original gel image; however, lanes intermediate to those shown have been removed for clarity or economy of presentation.

anti-angiogenic function (87). A number of genes not previously described as downregulated during adipogenesis were identified. Several are related to cell proliferation; this is expected, in that studies of in vitro adipogenesis indicate growth arrest to be a central step (40). These include Cdk4 (45), Cdc2 (29), proliferin-2 (22), and the receptor tyrosine kinase Axl (43). Aurora kinase B (Aurkb) (14) and Mtap1b, (74), are involved in microtubule dynamics. Microtubule dynamics play a role in the regulation of adipocyte lipid droplet size as well as insulin-stimulated GLUT4 translocation (9, 42,

78), and downregulation of Aurkb and Mtap1b may be related to these processes. Other newly identified genes downregulated in adipogenesis encode secreted factors. Igfbp6 is a member of the insulin-like growth factor binding protein family (30). Our finding that three anti-angiogenic secreted factors, Thbs2 (64), Serpinf1 (23), and Ccl2/MCP-1 (87), decrease on adipocyte conversion is consistent with this close link between angiogenesis and expansion of adipose tissue mass (48). The function of lysyl oxidase, Fkbp10, and Slc7a5 in adipogenesis remains to be investigated. In addition to those genes that were downregulated in both ScAP-23 and 3T3-L1 adipogenesis, filter analysis indicated that Gaa, Lgals1, and Hsp90aa1 were not decreased during 3T3-L1 adipogenesis; this transcript expression pattern was confirmed by real-time PCR (data not shown).

The contribution of the nonadipocyte component of adipose tissue to obesity and its related pathologies is recently emerging (21, 116). We therefore determined whether the preadipocyte-enriched genes were differentially expressed in obesity by performing real-time PCR analysis on RNA from subcutaneous WAT tissue from wild-type mice and from the murine *ob/ob* genetic model of obesity. As shown in Fig. 9, the expression level of transcripts for Thbs2, Ccl2, Aurkb, Slc7a5, and Serpinf1 was elevated in *ob/ob* WAT. Thbs2 evidenced the highest degree of upregulation in *ob/ob* WAT, with an average increase of approximately sevenfold; this is consistent with the recent report of upregulation of Thbs-2 in genetic and diet-induced murine models of obesity (114). An approximately twofold upregulation of a second anti-angiogenic factor, Serpinf1, is also noted in obesity. We also found an approximate fivefold increase in Ccl2/MCP-1 in obesity; this is consistent with that previously reported for this factor (11, 55). Proteins encoded by these genes may contribute to balance of the various pro- and anti-angiogenic factors involved in the growth/maintenance of adipose tissue mass. Approximately threefold and fivefold increases for Aurkb and Slc7a5 tran-

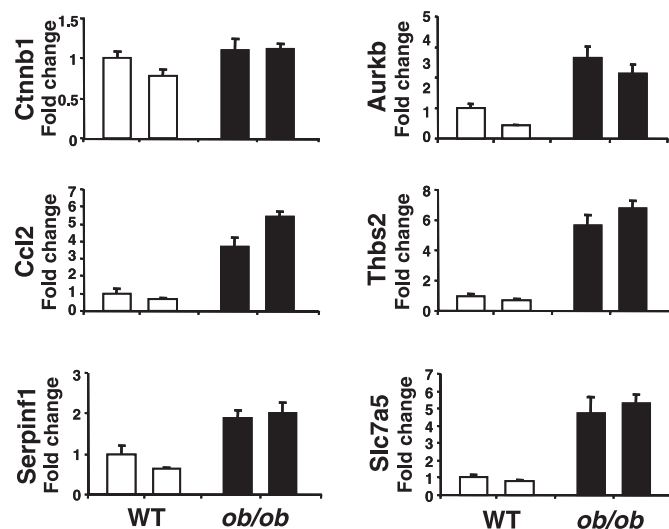


Fig. 9. Expression of Ctnnb1, Ccl2, Serpinf1, Aurkb, Thbs2, and Slc7a5 in adipose tissue of wild-type and *ob/ob* mice. Subcutaneous WAT RNA from 2 C57BL/6 wild-type mice (WT; open bars) and 2 *ob/ob* mice (solid bars) was collected, and real-time PCR was performed as described in MATERIALS AND METHODS. Values were normalized to Gapdh expression, and the gene expression level of the first WT bar was set at 1. Average fold changes were calculated and are shown as means \pm SD in triplicate.

scripts were also noted. A role, if any, of these latter two genes in obesity is yet to be determined.

Our studies on the molecular events of ScAP-23 adipogenesis to date have focused primarily on assessing gene expression distinctions in the preadipocyte vs. the mature adipocyte stage. Future analysis of this new adipogenesis model will address the interim stages of adipogenesis, including the early events of this process. With regard to this, the initial phase of adipocyte conversion of 3T3-L1 cells is termed mitotic clonal expansion (MCE) and is defined as two relatively rapid rounds of synchronous reentry into cell cycle mitoses. MCE is initiated on treatment of 2-day postconfluent preadipocytes, which have undergone density-dependent growth arrest in a unique G₀/G₁ state (71). MCE is initiated via extracellular signals from the differentiation inducers and is followed by expression of genes that lead to acquisition of the mature adipocyte phenotype (71). The MCE phase of 3T3-L1 adipogenesis was first documented ~25 years ago (96), and many key molecular details of this process that intimately tie cell cycle control to adipogenesis have been clarified in this model in the intervening years (79, 98, 99, 102, 123). MCE has been demonstrated to be requisite for adipogenesis of 3T3-L1 cells (101). Other *in vitro* adipogenesis models are far less well characterized with regard to MCE. For example, it appears unclear as to whether it is requisite for differentiation of the mesenchymal stem cells line, CH310T1/2 (18, 100). It has been reported that ST-13 preadipocytes, which derive from precursors present in adult mammary gland (120) and human primary preadipocytes (32), do not require MCE.

Given that ScAP-23 are not postconfluently growth arrested at the time of treatment with adipogenic inducers, but rather have just attained confluence, we presently believe that the strict definition of MCE developed from studies on 3T3-L1 adipogenesis does not apply to ScAP-23 cells. Two-day postconfluent ScAP-23 cells appear sickly with loss of morphological integrity. When we assessed cell number during the first 48 h of adipogenic induction, we failed to find an increase that was specific to treatment with adipogenic inducers and that would be indicative of MCE during early-stage ScAP-23 adipogenesis (data not shown). We have also observed a high degree of differentiation in individual underconfluent cells, indicating that confluence *per se* is not needed for adipogenesis of ScAP-23 preadipocytes, although underconfluent cells differentiate less uniformly. Agents that have been previously studied in adipogenesis have been identified to effectively substitute for postconfluence-induced growth arrest, for example, growth arrest via treatment with sodium butyrate (111). While not reported in the context of adipogenesis, indomethacin, the agent we identify as key to ScAP-23 adipogenesis, induces growth arrest in a number of other cell types (6, 25). It may be serving a similar function in ScAP-23 adipogenesis. It has been postulated that embryonic preadipocyte cell lines may require clonal expansion, whereas those that are adult derived may not (32), and that perhaps in these cases the critical mitoses of MCE, which are speculated to result in increased accessibility of key DNA regulatory regions, have already taken place *in vivo* (32). This may be the case for ScAP-23. Future studies can address in detail the temporal relationships between growth arrest and differentiation in this cell line.

Our analysis to date of gene expression in ScAP-23 and 3T3-L1 adipogenesis has allowed us to identify similarities and

distinctions at the preadipocyte and adipocyte stage, and future work can further define gene expression profiles of ScAP-23 preadipocytes and adipocytes. As such, our gene expression studies suggest the possibility of key distinctions in the molecular gene expression and differentiation machinery present in 3T3-L1 vs. ScAP-23 adipogenesis. It is not yet clear to what extent these molecular distinctions may reflect the different tissue origin of these two cells lines. It would also be of interest to determine to what degree the ScAP-23 model is reflective of adipogenesis that is specific to the subcutaneous WAT depot. Various studies in humans and rodents have illuminated distinctions in the physiology of adipocytes among the different WAT depots (5). In addition, preadipocytes from the individual WAT depots show depot-dependent characteristics (2, 26, 27, 34, 47, 59–61, 73, 76, 104, 106, 107, 115). These distinctions, and their molecular underpinnings, are gaining in importance with the realization that it is the anatomic location of excess adipose tissue that underlies the detrimental health impact of obesity (62). *In vitro* studies of subcutaneous and intra-abdominal preadipocytes have indicated regional variations in the capacity of precursors for replication (26, 59, 115), preadipocyte number (61), adipogenic differentiation (2, 27, 47, 59, 104), and susceptibility to apoptosis (107). Depot-dependent distinctions in expression level of select adipocyte differentiation marker genes have been identified (60, 68, 73, 76, 104). Moreover, recent application of DNA chip microarray technology has determined the transcriptional profiles of preadipocytes and adipocytes from distinct WAT depots and in cultures derived thereof (34, 106). These studies have uncovered the depot-dependent differential gene expression of Hox family genes and others with known roles in patterning and development (34, 106), as well as others. Interestingly, fat depot-specific cellular and gene expression characteristics are retained after culturing of primary preadipocytes and in cell strains obtained from single human preadipocytes (34, 104–106). Such observations led to the conclusions that aspects of depot-related preadipocyte gene expression are of an inherent and apparently cell-autonomous nature (34, 106). Overall, these recent studies have highlighted the fact that different WAT adipose depots should likely be regarded as distinct miniorgans (15). White preadipocytes/adipocytes also exist outside of discrete WAT depots, such as in bone marrow (35, 37, 66) and intramuscular (33), orbital (93), perivascularity (121), and epicardial (52) locations. It might be presumed that these cells may possess inherent distinctions and also share commonalities of function and gene expression that define each as fundamentally preadipocyte in nature. Thus it appears that, with regard to the molecular and cellular definition of the preadipocyte, the effects of adipose depot, as well as the *in vivo* vs. *in vitro* setting, come into play. The continuing analysis of ScAP-23 as well as other existing models, including newly emerging models derived from individual fat depots, should allow additional key insights into fundamental and depot-dependent aspects of preadipocyte biology.

ACKNOWLEDGMENTS

We thank Dr. Robert Weinberg (Massachusetts Institute of Technology, Cambridge, MA) for the pBabe-puro-hTERT retroviral expression construct.

GRANTS

This work was supported by National Institute of Diabetes and Digestive and Kidney Diseases Grant 5R21-DK-064992 to C. M. Smas.

REFERENCES

1. Abu-Abid S, Szold A, Klausner J. Obesity and cancer. *J Med* 33: 73–86, 2002.
2. Adams M, Montague CT, Prins JB, Holder JC, Smith SA, Sanders L, Digby JE, Sewter CP, Lazar MA, Chatterjee VK, O'Rahilly S. Activators of peroxisome proliferator-activated receptor gamma have depot-specific effects on human preadipocyte differentiation. *J Clin Invest* 100: 3149–3153, 1997.
3. Ailhaud G, Grimaldi P, Negrel R. Cellular and molecular aspects of adipose tissue development. *Annu Rev Nutr* 12: 207–233, 1992.
4. Aitman TJ, Glazier AM, Wallace CA, Cooper LD, Norsworthy PJ, Wahid FN, Al-Majali KM, Trembling PM, Mann CJ, Shoulders CC, Graf D, St Lezin E, Kurtz TW, Kren V, Pravenec M, Ibrahim A, Abumrad NA, Stanton LW, Scott J. Identification of Cd36 (Fat) as an insulin-resistance gene causing defective fatty acid and glucose metabolism in hypertensive rats. *Nat Genet* 21: 76–83, 1999.
5. Arner P. Regional adiposity in man. *J Endocrinol* 155: 191–192, 1997.
6. Bayer BM, Kruth HS, Vaughan M, Beaven MA. Arrest of cultured cells in the G1 phase of the cell cycle by indomethacin. *J Pharmacol Exp Ther* 210: 106–111, 1979.
7. Bernlohr DA, Angus CW, Lane MD, Bolanowski MA, Kelly TJ Jr. Expression of specific mRNAs during adipose differentiation: identification of an mRNA encoding a homologue of myelin P2 protein. *Proc Natl Acad Sci USA* 81: 5468–5472, 1984.
8. Bolduc C, Larose M, Lafond N, Yoshioka M, Rodrigue MA, Morissette J, Labrie C, Raymond V, St-Amand J. Adipose tissue transcriptome by serial analysis of gene expression. *Obes Res* 12: 750–757, 2004.
9. Bostrom P, Rutberg M, Ericsson J, Holmdahl P, Andersson L, Frohman MA, Boren J, Olofsson SO. Cytosolic lipid droplets increase in size by microtubule-dependent complex formation. *Arterioscler Thromb Vasc Biol* 25: 1945–1951, 2005.
10. Bradley RL, Cleveland KA, Cheatham B. The adipocyte as a secretory organ: mechanisms of vesicle transport and secretory pathways. *Recent Prog Horm Res* 56: 329–358, 2001.
11. Bruun JM, Lihn AS, Pedersen SB, Richelsen B. Monocyte chemoattractant protein-1 release is higher in visceral than subcutaneous human adipose tissue (AT): implication of macrophages resident in the AT. *J Clin Endocrinol Metab* 90: 2282–2289, 2005.
12. Calle EE, Kaaks R. Overweight, obesity and cancer: epidemiological evidence and proposed mechanisms. *Nat Rev Cancer* 4: 579–591, 2004.
13. Campfield LA, Smith FJ, Burn P. Strategies and potential molecular targets for obesity treatment. *Science* 280: 1383–1387, 1998.
14. Carmena M, Earnshaw WC. The cellular geography of aurora kinases. *Nat Rev Mol Cell Biol* 4: 842–854, 2003.
15. Caserta F, Tchkonja T, Civelek VN, Prentki M, Brown NF, McGarry JD, Forse RA, Corkey BE, Hamilton JA, Kirkland JL. Fat depot origin affects fatty acid handling in cultured rat and human preadipocytes. *Am J Physiol Endocrinol Metab* 280: E238–E247, 2001.
16. Chang JK, Wang GJ, Tsai ST, Ho ML. Nonsteroidal anti-inflammatory drug effects on osteoblastic cell cycle, cytotoxicity, and cell death. *Connect Tissue Res* 46: 200–210, 2005.
17. Chen Z, Torrens JI, Anand A, Spiegelman BM, Friedman JM. Krox20 stimulates adipogenesis via C/EBPbeta-dependent and -independent mechanisms. *Cell Metab* 1: 93–106, 2005.
18. Cho YC, Jefcoate CR. PPARgamma1 synthesis and adipogenesis in C3H10T1/2 cells depends on S-phase progression, but does not require mitotic clonal expansion. *J Cell Biochem* 91: 336–353, 2004.
19. Cinti S. Adipocyte differentiation and transdifferentiation: plasticity of the adipose organ. *J Endocrinol Invest* 25: 823–835, 2002.
20. Cook KS, Min HY, Johnson D, Chaplinsky RJ, Flier JS, Hunt CR, Spiegelman BM. Adipsin: a circulating serine protease homolog secreted by adipose tissue and sciatic nerve. *Science* 237: 402–405, 1987.
21. Coppack SW. Pro-inflammatory cytokines and adipose tissue. *Proc Nutr Soc* 60: 349–356, 2001.
22. Corbacho AM, Martinez De La Escalera G, Clapp C. Roles of prolactin and related members of the prolactin/growth hormone/placental lactogen family in angiogenesis. *J Endocrinol* 173: 219–238, 2002.
23. Dawson DW, Volpert OV, Gillis P, Crawford SE, Xu H, Benedict W, Bouck NP. Pigment epithelium-derived factor: a potent inhibitor of angiogenesis. *Science* 285: 245–248, 1999.
24. Dennis JE, Merriam A, Awadallah A, Yoo JU, Johnstone B, Caplan AI. A quadripotential mesenchymal progenitor cell isolated from the marrow of an adult mouse. *J Bone Miner Res* 14: 700–709, 1999.
25. Detjen KM, Welzel M, Wiedenmann B, Rosewicz S. Nonsteroidal anti-inflammatory drugs inhibit growth of human neuroendocrine tumor cells via G1 cell-cycle arrest. *Int J Cancer* 107: 844–853, 2003.
26. Djian P, Roncari AK, Hollenberg CH. Influence of anatomic site and age on the replication and differentiation of rat adipocyte precursors in culture. *J Clin Invest* 72: 1200–1208, 1983.
27. Djian P, Roncari DA, Hollenberg CH. Adipocyte precursor clones vary in capacity for differentiation. *Metabolism* 34: 880–883, 1985.
28. Doi H, Masaki N, Takahashi H, Komatsu H, Fujimori K, Satomi S. A new preadipocyte cell line, AP-18, established from adult mouse adipose tissue. *Tohoku J Exp Med* 207: 209–216, 2005.
29. Draetta G, Pivnicka-Worms H, Morrison D, Druker B, Roberts T, Beach D. Human cdc2 protein kinase is a major cell-cycle regulated tyrosine kinase substrate. *Nature* 336: 738–744, 1988.
30. Ehrenborg E, Zazzi H, Lagercrantz S, Granqvist M, Hillerbrand U, Allander SV, Larsson C, Luthman H. Characterization and chromosomal localization of the human insulin-like growth factor-binding protein 6 gene. *Mamm Genome* 10: 376–380, 1999.
31. Endemann G, Stanton LW, Madden KS, Bryant CM, White RT, Protter AA. CD36 is a receptor for oxidized low density lipoprotein. *J Biol Chem* 268: 11811–11816, 1993.
32. Entenmann G, Hauner H. Relationship between replication and differentiation in cultured human adipocyte precursor cells. *Am J Physiol Cell Physiol* 270: C1011–C1016, 1996.
33. Gallagher D, Kuznia P, Heshka S, Albu J, Heymsfield SB, Goodpaster B, Visser M, Harris TB. Adipose tissue in muscle: a novel depot similar in size to visceral adipose tissue. *Am J Clin Nutr* 81: 903–910, 2005.
34. Gesta S, Blüher M, Yamamoto Y, Norris AW, Berndt J, Kralisch S, Boucher J, Lewis C, Kahn CR. Evidence for a role of developmental genes in the origin of obesity and body fat distribution. *Proc Natl Acad Sci USA* 103: 6676–6681, 2006.
35. Gimble JM, Dorheim MA, Cheng Q, Pekala P, Enerback S, Ellingsworth L, Kincade PW, Wang CS. Response of bone marrow stromal cells to adipogenic antagonists. *Mol Cell Biol* 9: 4587–4595, 1989.
36. Gimble JM, Guilak F. Differentiation potential of adipose derived adult stem (ADAS) cells. *Curr Top Dev Biol* 58: 137–160, 2003.
37. Gimble JM, Youkhana K, Hua X, Bass H, Medina K, Sullivan M, Greenberger J, Wang CS. Adipogenesis in a myeloid supporting bone marrow stromal cell line. *J Cell Biochem* 50: 73–82, 1992.
38. Green H, Kehinde O. An established preadipose cell line and its differentiation in culture. II. Factors affecting the adipose conversion. *Cell* 5: 19–27, 1975.
39. Gregoire FM. Adipocyte differentiation: from fibroblast to endocrine cell. *Exp Biol Med (Maywood)* 226: 997–1002, 2001.
40. Gregoire FM, Smas CM, Sul HS. Understanding adipocyte differentiation. *Physiol Rev* 78: 783–809, 1998.
41. Guilak F, Lott KE, Awad HA, Cao Q, Hicok KC, Fermor B, Gimble JM. Clonal analysis of the differentiation potential of human adipose-derived adult stem cells. *J Cell Physiol* 206: 229–237, 2006.
42. Guilherme A, Emoto M, Buxton JM, Bose S, Sabini R, Theurkauf WE, Leszyk J, Czech MP. Perinuclear localization and insulin responsiveness of GLUT4 requires cytoskeletal integrity in 3T3-L1 adipocytes. *J Biol Chem* 275: 38151–38159, 2000.
43. Hafizi S, Dahlback B. Signalling and functional diversity within the Axl subfamily of receptor tyrosine kinases. *Cytokine Growth Factor Rev* 17: 295–304, 2006.
44. Hansen JB, Jorgensen C, Petersen RK, Hallenborg P, De Matteis R, Boye HA, Petrovic N, Enerback S, Nedergaard J, Cinti S, te Riele H, Kristiansen K. Retinoblastoma protein functions as a molecular switch determining white versus brown adipocyte differentiation. *Proc Natl Acad Sci USA* 101: 4112–4117, 2004.
45. Harbour JW, Luo RX, Dei Santi A, Postigo AA, Dean DC. Cdk phosphorylation triggers sequential intramolecular interactions that progressively block Rb functions as cells move through G1. *Cell* 98: 859–869, 1999.
46. Harp JB. New insights into inhibitors of adipogenesis. *Curr Opin Lipidol* 15: 303–307, 2004.
47. Hauner H, Entenmann G. Regional variation of adipose differentiation in cultured stromal-vascular cells from the abdominal and femoral adipose tissue of obese women. *Int J Obes* 15: 121–126, 1991.
48. Hausman GJ, Richardson RL. Adipose tissue angiogenesis. *J Anim Sci* 82: 925–934, 2004.

49. **Hiragun A, Sato M, Mitsui H.** Establishment of a clonal cell line that differentiates into adipose cells in vitro. *In Vitro* 16: 685–693, 1980.
50. **Hu E, Liang P, Spiegelman BM.** AdipoQ is a novel adipose-specific gene dysregulated in obesity. *J Biol Chem* 271: 10697–10703, 1996.
51. **Hugo ER, Brandebourg TD, Comstock CE, Gersin KS, Sussman JJ, Ben-Jonathan N.** LS14: a novel human adipocyte cell line that produces prolactin. *Endocrinology* 147: 306–313, 2006.
52. **Iacobellis G, Corradi D, Sharma AM.** Epicardial adipose tissue: anatomic, biomolecular and clinical relationships with the heart. *Nat Clin Pract Cardiovasc Med* 2: 536–543, 2005.
53. **Jessen BA, Stevens GJ.** Expression profiling during adipocyte differentiation of 3T3-L1 fibroblasts. *Gene* 299: 95–100, 2002.
54. **Jong MC, Voshol PJ, Muurling M, Dahlmans VE, Romijn JA, Pijl H, Havekes LM.** Protection from obesity and insulin resistance in mice overexpressing human apolipoprotein C1. *Diabetes* 50: 2779–2785, 2001.
55. **Kanda H, Tateya S, Tamori Y, Kotani K, Hiasa K, Kitazawa R, Kitazawa S, Miyachi H, Maeda S, Egashira K, Kasuga M.** MCP-1 contributes to macrophage infiltration into adipose tissue, insulin resistance, and hepatic steatosis in obesity. *J Clin Invest* 116: 1494–1505, 2006.
56. **Katsuno M, Motomura S, Kaneko S, Sakai H, Ibayashi H.** A preadipocyte cell line derived from murine bone marrow stroma: characterization of morphological, enzymatic, and functional nature of the cells. *Int J Cell Cloning* 3: 81–90, 1985.
57. **Kim JB, Spiegelman BM.** ADD1/SREBP1 promotes adipocyte differentiation and gene expression linked to fatty acid metabolism. *Genes Dev* 10: 1096–1107, 1996.
58. **Kim S, Moustaid-Moussa N.** Secretory, endocrine and autocrine/paracrine function of the adipocyte. *J Nutr* 130: 3110S–3115S, 2000.
59. **Kirkland JL, Hollenberg CH, Gillon WS.** Age, anatomic site, and the replication and differentiation of adipocyte precursors. *Am J Physiol Cell Physiol* 258: C206–C210, 1990.
60. **Kirkland JL, Hollenberg CH, Gillon WS.** Effects of fat depot site on differentiation-dependent gene expression in rat preadipocytes. *Int J Obes Relat Metab Disord* 20, Suppl 3: S102–S107, 1996.
61. **Kirkland JL, Hollenberg CH, Kindler S, Gillon WS.** Effects of age and anatomic site on preadipocyte number in rat fat depots. *J Gerontol* 49: B31–B35, 1994.
62. **Kissebah AH, Krakower GR.** Regional adiposity and morbidity. *Physiol Rev* 74: 761–811, 1994.
63. **Kusunoki J, Kanatani A, Moller DE.** Modulation of fatty acid metabolism as a potential approach to the treatment of obesity and the metabolic syndrome. *Endocrine* 29: 91–100, 2006.
64. **Lahav J.** The functions of thrombospondin and its involvement in physiology and pathophysiology. *Biochim Biophys Acta* 1182: 1–14, 1993.
65. **Lanningham-Foster L, Green CL, Langkamp-Henken B, Davis BA, Nguyen KT, Bender BS, Cousins RJ.** Overexpression of CRIP in transgenic mice alters cytokine patterns and the immune response. *Am J Physiol Endocrinol Metab* 282: E1197–E1203, 2002.
66. **Lanotte M, Scott D, Dexter TM, Allen TD.** Clonal preadipocyte cell lines with different phenotypes derived from murine marrow stroma: factors influencing growth and adipogenesis in vitro. *J Cell Physiol* 111: 177–186, 1982.
67. **Lazar MA.** PPARgamma, 10 years later. *Biochimie* 87: 9–13, 2005.
68. **Lefebvre AM, Laville M, Vega N, Riou JP, van Gaal L, Auwerx J, Vidal H.** Depot-specific differences in adipose tissue gene expression in lean and obese subjects. *Diabetes* 47: 98–103, 1998.
69. **Lehmann JM, Lenhard JM, Oliver BB, Ringold GM, Kliewer SA.** Peroxisome proliferator-activated receptors alpha and gamma are activated by indomethacin and other non-steroidal anti-inflammatory drugs. *J Biol Chem* 272: 3406–3410, 1997.
70. **Lin Y, Chen X, Yan Z, Liu L, Tang W, Zheng X, Li Z, Qiao J, Li S, Tian W.** Multilineage differentiation of adipose-derived stromal cells from GFP transgenic mice. *Mol Cell Biochem* 285: 69–78, 2006.
71. **MacDougald OA, Lane MD.** Transcriptional regulation of gene expression during adipocyte differentiation. *Annu Rev Biochem* 64: 345–373, 1995.
72. **MacDougald OA, Mandrup S.** Adipogenesis: forces that tip the scales. *Trends Endocrinol Metab* 13: 5–11, 2002.
73. **Masuzaki H, Ogawa Y, Isse N, Satoh N, Okazaki T, Shigemoto M, Mori K, Tamura N, Hosoda K, Yoshimasa Y, et al.** Human obese gene expression. Adipocyte-specific expression and regional differences in the adipose tissue. *Diabetes* 44: 855–858, 1995.
74. **Meixner A, Haverkamp S, Wasse H, Fuhrer S, Thalhammer J, Kropf N, Bittner RE, Lassmann H, Wiche G, Propst F.** MAP1B is required for axon guidance and is involved in the development of the central and peripheral nervous system. *J Cell Biol* 151: 1169–1178, 2000.
75. **Moldes M, Lasnier F, Feve B, Pairault J, Djian P.** Id3 prevents differentiation of preadipose cells. *Mol Cell Biol* 17: 1796–1804, 1997.
76. **Montague CT, Prins JB, Sanders L, Digby JE, O'Rahilly S.** Depot- and sex-specific differences in human leptin mRNA expression: implications for the control of regional fat distribution. *Diabetes* 46: 342–347, 1997.
77. **Negrel R, Grimaldi P, Ailhaud G.** Establishment of preadipocyte clonal line from epididymal fat pad of ob/ob mouse that responds to insulin and to lipolytic hormones. *Proc Natl Acad Sci USA* 75: 6054–6058, 1978.
78. **Olson AL, Trumbly AR, Gibson GV.** Insulin-mediated GLUT4 translocation is dependent on the microtubule network. *J Biol Chem* 276: 10706–10714, 2001.
79. **Patel YM, Lane MD.** Mitotic clonal expansion during preadipocyte differentiation: calpain-mediated turnover of p27. *J Biol Chem* 275: 17653–17660, 2000.
80. **Pittenger MF, Mackay AM, Beck SC, Jaiswal RK, Douglas R, Mosca JD, Moorman MA, Simonetti DW, Craig S, Marshak DR.** Multilineage potential of adult human mesenchymal stem cells. *Science* 284: 143–147, 1999.
81. **Rosen ED.** The transcriptional basis of adipocyte development. *Prostaglandins Leukot Essent Fatty Acids* 73: 31–34, 2005.
82. **Rosen ED, Spiegelman BM.** Molecular regulation of adipogenesis. *Annu Rev Cell Dev Biol* 16: 145–171, 2000.
83. **Ross SE, Erickson RL, Gerin I, DeRose PM, Bajnok L, Longo KA, Misk DE, Kuick R, Hanash SM, Atkins KB, Andresen SM, Nebb HI, Madsen L, Kristiansen K, MacDougald OA.** Microarray analyses during adipogenesis: understanding the effects of Wnt signaling on adipogenesis and the roles of liver X receptor alpha in adipocyte metabolism. *Mol Cell Biol* 22: 5989–5999, 2002.
84. **Ross SE, Hemati N, Longo KA, Bennett CN, Lucas PC, Erickson RL, MacDougald OA.** Inhibition of adipogenesis by Wnt signaling. *Science* 289: 950–953, 2000.
85. **Ruan H, Zarnowski MJ, Cushman SW, Lodish HF.** Standard isolation of primary adipose cells from mouse epididymal fat pads induces inflammatory mediators and down-regulates adipocyte genes. *J Biol Chem* 278: 47585–47593, 2003.
86. **Safford KM, Safford SD, Gimble JM, Shetty AK, Rice HE.** Characterization of neuronal/glial differentiation of murine adipose-derived adult stromal cells. *Exp Neurol* 187: 319–328, 2004.
87. **Salcedo R, Ponce ML, Young HA, Wasserman K, Ward JM, Kleinman HK, Oppenheim JJ, Murphy WJ.** Human endothelial cells express CCR2 and respond to MCP-1: direct role of MCP-1 in angiogenesis and tumor progression. *Blood* 96: 34–40, 2000.
88. **Saye JA, Cassis LA, Sturgill TW, Lynch KR, Peach MJ.** Angiotensinogen gene expression in 3T3-L1 cells. *Am J Physiol Cell Physiol* 256: C448–C451, 1989.
89. **Shi H, Tzameli I, Bjorbaek C, Flier JS.** Suppressor of cytokine signaling 3 is a physiological regulator of adipocyte insulin signaling. *J Biol Chem* 279: 34733–34740, 2004.
90. **Shimomura I, Hammer RE, Richardson JA, Ikemoto S, Bashmakov Y, Goldstein JL, Brown MS.** Insulin resistance and diabetes mellitus in transgenic mice expressing nuclear SREBP-1c in adipose tissue: model for congenital generalized lipodystrophy. *Genes Dev* 12: 3182–3194, 1998.
91. **Smas CM, Sul HS.** Pref-1, a protein containing EGF-like repeats, inhibits adipocyte differentiation. *Cell* 73: 725–734, 1993.
92. **Smith ML, Hawcroft G, Hull MA.** The effect of non-steroidal anti-inflammatory drugs on human colorectal cancer cells: evidence of different mechanisms of action. *Eur J Cancer* 36: 664–674, 2000.
93. **Sorisky A, Pardasani D, Gagnon A, Smith TJ.** Evidence of adipocyte differentiation in human orbital fibroblasts in primary culture. *J Clin Endocrinol Metab* 81: 3428–3431, 1996.
94. **Soukas A, Succi ND, Saatkamp BD, Novelli S, Friedman JM.** Distinct transcriptional profiles of adipogenesis in vivo and in vitro. *J Biol Chem* 276: 34167–34174, 2001.
95. **Spiegelman BM, Frank M, Green H.** Molecular cloning of mRNA from 3T3 adipocytes. Regulation of mRNA content for glycerophosphate

- dehydrogenase and other differentiation-dependent proteins during adipocyte development. *J Biol Chem* 258: 10083–10089, 1983.
96. **Student AK, Hsu RY, Lane MD.** Induction of fatty acid synthetase synthesis in differentiating 3T3-L1 preadipocytes. *J Biol Chem* 255: 4745–4750, 1980.
 97. **Taleb S, Lacasa D, Bastard JP, Poitou C, Cancello R, Pelloux V, Viguerie N, Benis A, Zucker JD, Bouillot JL, Coussieu C, Basdevant A, Langin D, Clement K.** Cathepsin S, a novel biomarker of adiposity: relevance to atherogenesis. *FASEB J* 19: 1540–1542, 2005.
 98. **Tang QQ, Gronborg M, Huang H, Kim JW, Otto TC, Pandey A, Lane MD.** Sequential phosphorylation of CCAAT enhancer-binding protein beta by MAPK and glycogen synthase kinase 3beta is required for adipogenesis. *Proc Natl Acad Sci USA* 102: 9766–9771, 2005.
 99. **Tang QQ, Lane MD.** Activation and centromeric localization of CCAAT/enhancer-binding proteins during the mitotic clonal expansion of adipocyte differentiation. *Genes Dev* 13: 2231–2241, 1999.
 100. **Tang QQ, Otto TC, Lane MD.** Commitment of C3H10T1/2 pluripotent stem cells to the adipocyte lineage. *Proc Natl Acad Sci USA* 101: 9607–9611, 2004.
 101. **Tang QQ, Otto TC, Lane MD.** Mitotic clonal expansion: a synchronous process required for adipogenesis. *Proc Natl Acad Sci USA* 100: 44–49, 2003.
 102. **Tao H, Umek RM.** C/EBPalpha is required to maintain postmitotic growth arrest in adipocytes. *DNA Cell Biol* 19: 9–18, 2000.
 103. **Taylor SM, Jones PA.** Multiple new phenotypes induced in 10T1/2 and 3T3 cells treated with 5-azacytidine. *Cell* 17: 771–779, 1979.
 104. **Tchkonina T, Giorgadze N, Pirtskhalava T, Tchoukalova Y, Karagiannides I, Forse RA, DePonte M, Stevenson M, Guo W, Han J, Waloga G, Lash TL, Jensen MD, Kirkland JL.** Fat depot origin affects adipogenesis in primary cultured and cloned human preadipocytes. *Am J Physiol Regul Integr Comp Physiol* 282: R1286–R1296, 2002.
 105. **Tchkonina T, Giorgadze N, Pirtskhalava T, Thomou T, DePonte M, Koo A, Forse RA, Chinnappan D, Martin-Ruiz C, von Zglinicki T, Kirkland JL.** Fat depot-specific characteristics are retained in strains derived from single human preadipocytes. *Diabetes* 55: 2571–2578, 2006.
 106. **Tchkonina T, Lenburg M, Thomou T, Giorgadze N, Frampton G, Pirtskhalava T, Cartwright A, Cartwright M, Flanagan J, Karagiannides I, Gerry N, Forse RA, Tchoukalova Y, Jensen MD, Pothoulakis C, Kirkland JL.** Identification of depot-specific human fat cell progenitors through distinct expression profiles and developmental gene patterns. *Am J Physiol Endocrinol Metab* 292: E298–E307, 2007.
 107. **Tchkonina T, Tchoukalova YD, Giorgadze N, Pirtskhalava T, Karagiannides I, Forse RA, Koo A, Stevenson M, Chinnappan D, Cartwright A, Jensen MD, Kirkland JL.** Abundance of two human preadipocyte subtypes with distinct capacities for replication, adipogenesis, and apoptosis varies among fat depots. *Am J Physiol Endocrinol Metab* 288: E267–E277, 2005.
 108. **Tong Q, Dalgin G, Xu H, Ting CN, Leiden JM, Hotamisligil GS.** Function of GATA transcription factors in preadipocyte-adipocyte transition. *Science* 290: 134–138, 2000.
 109. **Tontonoz P, Hu E, Spiegelman BM.** Regulation of adipocyte gene expression and differentiation by peroxisome proliferator activated receptor gamma. *Curr Opin Genet Dev* 5: 571–576, 1995.
 110. **Torii I, Morikawa S, Nakano A, Morikawa K.** Establishment of a human preadipose cell line, HPB-AML-I: refractory to PPARgamma-mediated adipogenic stimulation. *J Cell Physiol* 197: 42–52, 2003.
 111. **Toscani A, Soprano DR, Soprano KJ.** Sodium butyrate in combination with insulin or dexamethasone can terminally differentiate actively proliferating Swiss 3T3 cells into adipocytes. *J Biol Chem* 265: 5722–5730, 1990.
 112. **Umek RM, Friedman AD, McKnight SL.** CCAAT-enhancer binding protein: a component of a differentiation switch. *Science* 251: 288–292, 1991.
 113. **Van Schothorst EM, Franssen-van Hal N, Schaap MM, Pennings J, Hoebee B, Keijer J.** Adipose gene expression patterns of weight gain suggest counteracting steroid hormone synthesis. *Obes Res* 13: 1031–1041, 2005.
 114. **Voros G, Maquoi E, Demeulemeester D, Clerx N, Collen D, Lijnen HR.** Modulation of angiogenesis during adipose tissue development in murine models of obesity. *Endocrinology* 146: 4545–4554, 2005.
 115. **Wang H, Kirkland JL, Hollenberg CH.** Varying capacities for replication of rat adipocyte precursor clones and adipose tissue growth. *J Clin Invest* 83: 1741–1746, 1989.
 116. **Weisberg SP, McCann D, Desai M, Rosenbaum M, Leibel RL, Ferrante AW Jr.** Obesity is associated with macrophage accumulation in adipose tissue. *J Clin Invest* 112: 1796–1808, 2003.
 117. **Wellen KE, Hotamisligil GS.** Inflammation, stress, and diabetes. *J Clin Invest* 115: 1111–1119, 2005.
 118. **Xu H, Barnes GT, Yang Q, Tan G, Yang D, Chou CJ, Sole J, Nichols A, Ross JS, Tartaglia LA, Chen H.** Chronic inflammation in fat plays a crucial role in the development of obesity-related insulin resistance. *J Clin Invest* 112: 1821–1830, 2003.
 119. **Yagi K, Kondo D, Okazaki Y, Kano K.** A novel preadipocyte cell line established from mouse adult mature adipocytes. *Biochem Biophys Res Commun* 321: 967–974, 2004.
 120. **Yajima Y, Sato M, Sorimachi H, Inomata M, Maki M, Kawashima S.** Calpain system regulates the differentiation of adult primitive mesenchymal ST-13 adipocytes. *Endocrinology* 147: 4811–4819, 2006.
 121. **Yudkin JS, Eringa E, Stehouwer CD.** “Vasocrine” signalling from perivascular fat: a mechanism linking insulin resistance to vascular disease. *Lancet* 365: 1817–1820, 2005.
 122. **Zechner R, Newman TC, Sherry B, Cerami A, Breslow JL.** Recombinant human cachectin/tumor necrosis factor but not interleukin-1 alpha downregulates lipoprotein lipase gene expression at the transcriptional level in mouse 3T3-L1 adipocytes. *Mol Cell Biol* 8: 2394–2401, 1988.
 123. **Zhang JW, Tang QQ, Vinson C, Lane MD.** Dominant-negative C/EBP disrupts mitotic clonal expansion and differentiation of 3T3-L1 preadipocytes. *Proc Natl Acad Sci USA* 101: 43–47, 2004.
 124. **Zheng B, Cao B, Li G, Huard J.** Mouse adipose-derived stem cells undergo multilineage differentiation in vitro but primarily osteogenic and chondrogenic differentiation in vivo. *Tissue Eng* 12: 1891–1901, 2006.
 125. **Zhou YT, Wang ZW, Higa M, Newgard CB, Unger RH.** Reversing adipocyte differentiation: implications for treatment of obesity. *Proc Natl Acad Sci USA* 96: 2391–2395, 1999.
 126. **Zuk PA, Zhu M, Ashjian P, De Ugarte DA, Huang JI, Mizuno H, Alfonso ZC, Fraser JK, Benhaim P, Hedrick MH.** Human adipose tissue is a source of multipotent stem cells. *Mol Biol Cell* 13: 4279–4295, 2002.